Bovine Nebovirus Interacts with a Wide Spectrum of Histo-Blood Group Antigens

Eun-Hyo Cho, Mahmoud Soliman, Mia Madel Alfajaro, Ji-Yun Kim, Ja-Young Seo, Jun-Gyu Park, Deok-Song Kim, Yeong-Bin Baek, Mun-Il Kang, Sang-Ik Park, et al.

Bovine Nebovirus Interacts with a Wide Spectrum of Histo-Blood Group Antigens

Eun-Hyo Cho,[a#] Mahmoud Soliman,[a#] Mia Madel Alfajaro,[a] Ji-Yun Kim,[a] Ja-Young Seo,[a] Jun-Gyu Park,[a] Deok-Song Kim,[a] Yeong-Bin Baek,[a] Mun-Il Kang,[a] Sang-Ik Park,[a] Jacques Le Pendu,[b*] Kyoung-Oh Cho[a*]

Laboratory of Veterinary Pathology, College of Veterinary Medicine, Chonnam National University, Gwangju, Republic of Korea[a]; CRCINA, Inserm, Université d'Angers, Université de Nantes, Nantes, France[b]

Running title: The Wide HBGA Binding Specificity of BNeV

*Corresponding authors: Jacques Le Pendu, Jacques.le-pendu@inserm.fr, and Kyoung-Oh Cho, choko@chonnam.ac.kr.

[#]E-H.C. and M.S. contributed equally to this paper.

ABSTRACT Some viruses within the *Caliciviridae* family initiate their replication cycle by attachment to cell surface carbohydrate moieties, histo-blood group antigens (HBGAs) and/or terminal sialic acids (SAs). Although bovine nebovirus (BNeV), one of the enteric caliciviruses, is an important causative agent of acute gastroenteritis in cattle, its attachment factors and possibly other cellular receptors remain unknown. Using a comprehensive series of protein-ligand biochemical assays, we sought to determine whether BNeV recognizes cell surface HBGAs and/or SAs as attachment factors. It was found that BNeV virus-like particles (VLPs) bound to A type/H type 2/Le^{y} HBGAs expressed in the bovine digestive tract which are related to HBGAs expressed in humans and other host species, suggesting a wide spectrum of HBGA recognition by BNeV. BNeV VLPs also bound to large variety of different bovine and human saliva samples of all ABH and Lewis types, supporting previously obtained results and suggesting a zoonotic potential of BNeV transmission. Removal of α1,2-linked-fucose and α1,3/4-linked-fucose epitopes of target HBGAs by confirmation-specific enzymes reduced the binding of BNeV VLPs to synthetic HBGAs, bovine and human saliva, cultured cell lines and bovine small intestine mucosa, further supporting a wide HBGA binding spectrum of BNeV through recognition of α1,2-linked-fucose and α1,3/4-linked-fucose epitopes of targeted HBGAs. However, removal of terminal α2,3- and α2,6-linked SAs by their specific enzyme had no inhibitory effects on binding of BNeV VLPs, indicating that BNeV does not use terminal SAs as attachment factors. Further details of the binding specificity of BNeV remain to be explored.

IMPORTANCE Enteric caliciviruses such as noroviruses, sapoviruses, and recoviruses are the most important etiological agents of severe acute gastroenteritis in humans and many other mammalian host species. They initiate infection by attachment to cell surface carbohydrate moieties, histo-blood group antigens (HBGAs) and/or terminal sialic acids (SAs). However, the attachment factor(s) for bovine nebovirus (BNeV), a recently classified enteric calicivirus genus/type species, remains unexplored. Here, we demonstrate that BNeV virus-like particles (VLPs) have a wide spectrum of binding to synthetic HBGAs, bovine and human saliva samples, and bovine duodenal sections. We further discovered that α1,2-linked-fucose and α1,3/4-linked-fucose epitopes are essential for binding of BNeV VLPs. However, BNeV VLPs do not bind to terminal SAs on cell carbohydrates. Continued investigation regarding the proteinaceous receptor(s) will be necessary for better understanding of the tropism, pathogenesis and host range of this important viral genus.

KEYWORDS Nebovirus, bovine calicivirus, attachment factor, HBGAs, binding spectrum, fucose

The binding of an infectious virus particle through attachment factors and receptors on the host cell surface is the essential first step for the viral entry and subsequent replication therein (1, 2). Generally, attachment factors facilitate the concentration of the incoming virus particles on the cell surface but do not actively promote entry and mediate signals, whereas receptors bind the viruses, promote entry, and activate cellular signaling pathways (3). Viral attachment factors and receptors on host cells comprise a large variety of proteins, carbohydrates, and lipids with physiological functions unrelated to pathogen interaction (3). For many viruses, these receptors are glycans linked to either a protein (glycoprotein or proteoglycan) or a glycolipid (4–6). Glycan-dependent viruses use glycoepitopes as receptors, binding to negatively charged sialic acids (SAs), sulfated oligosaccharide motifs of glycosaminoglycan (GAG) chains, or neutral glycoepitopes such as found on histo-blood group antigens (HBGAs) (6). SAs at the termini or inner portions of glycan chains serve as receptors for at least ten different virus families, whereas representatives from at least eight different virus families use GAG chains as receptors (4–7). In contrast, only a few human and animal viruses within a few families including *Caliciviridae*, *Parvoviridae*, and *Reoviridae* use HBGAs as receptors (2, 6, 8). The selection of different glycoepitopes as attachment factors may contribute to virus tropism, pathogenesis, and host specificity (5, 6, 8, 9).

Viruses within the family *Caliciviridae* are small, non-enveloped, icosahedral viruses that possess single-stranded, positive-sense genomic RNA of 7–8 kb in size (10). This family contains five established genera, *Lagovirus*, *Nebovirus*, *Norovirus*, *Sapovirus*, and *Vesivirus* (11). Recently, six additional unclassified caliciviruses may represent new genera tentatively named *Bavovirus* (12, 13), *Nacovirus* (13–15), *Recovirus* (16), *Salovirus* (17), *Sanovirus* (18), and *Valovirus* (19). Caliciviruses are important etiologic agents in humans and animals,

causing a variety of diseases in their respective hosts, such as respiratory disease (feline calicivirus [FCV]), hemorrhagic disease (rabbit hemorrhagic disease virus [RHDV]), and gastroenteritis (norovirus [NoV], sapovirus [SaV], and nebovirus [NeV]).

Several caliciviruses utilize cell surface carbohydrate moieties, SAs or HBGAs as attachment factors (2). The initial observation that the *Lagovirus* RHDV uses the H type 2 HBGA as an attachment factor (20) inspired studies to identify similar factors for the other members of the *Caliciviridae* family (21). These studies showed that different HBGAs are used as attachment factors for human NoVs (HuNoVs) (21, 22), bovine NoV (23), canine NoVs (24), and primate enteric caliciviruses within the *Recovirus* genus (25). In contrast, FCV (26), murine NoV (MNV) (27), and porcine SaV (PSaV) (28) utilize terminal SAs as attachment factors. Recently, it was observed that some HuNoVs and monkey recoviruses may also utilize SAs as attachment factors (29, 30). Finally, proteinaceous cellular surface structures were identified as receptors for a few caliciviruses, such as CD300lf and CD300ld for MNV (31, 32) and junctional adhesion molecule-1 (JAM-1) for FCV and Hom-1 calicivirus (33–35).

HBGAs are complex carbohydrates linked to glycoproteins or glycolipids found in red blood cells and epithelial cells of the gastrointestinal, genitourinary, and respiratory tracts in a wide variety of species (2, 8). They can also be secreted as free oligosaccharides into bodily fluids, such as saliva, intestinal content, milk, and blood (2, 8). The ABH and Lewis HBGAs are synthesized by the stepwise addition of monosaccharide units to five different types of precursor: type 1 (Galβ-3GlcNAcβ1-R), type 2 (Galβ-4GlcNAcβ1-R), type 3 (Galβ-3GalNAcα1-R), type 4 (Galβ-3GalNAcβ1-R), and type 5 (Galβ-4Glcβ1-Cer) (36). Each step is catalyzed by specific glycosyltransferases, such as α-1,2 fucosyltransferase (FUT2), α-1,3

or α-1,4 fucosyltransferase (FUT3), and two glycosyltransferases (A and B enzymes) (2, 8). For example, the α-1,2 fucosyltransferase adds a fucose residue at the α-1,2 linkage position of galactose, generating H antigen motifs (2, 8). The addition of N-acetylgalactosamine (GalNAc) or galactose at the α-1,3 position of H type chains via A enzyme or B enzyme respectively results in either A or B antigen (2, 8, 24). The *FUT3* gene, as well as the *FUT4*, *FUT5*, *FUT6*, *FUT7*, or *FUT9* genes, generate the Lewis antigens by adding a fucose residue at either the α-1,3 or α-1,4 linkage position of the N-acetylglucosamine (GlcNAc) in the type 1 and/or type 2 precursors (2, 8, 24).

The genus *Nebovirus* contains one established type species, Newbury-1 virus that contains Nebraska-like and Newbury1-like clades (37, 38). Recently, two more species in the genus *Nebovirus* have been identified (39, 40). The reported fecal prevalence of the bovine nebovirus (BNeV) in calf diarrhea is 5% in Tunisia (41), 4.8% in Brazil (42), 7% in France (40), 9.1% in Korea (38), 13.1% in Italy (43), and 21.6% in the United States (44). Moreover, the BNeV prototype strains Newbury1 and Nebraska experimentally induce diarrhea and small intestinal pathology such as the desquamation of villous epithelial cells and villous atrophy in gnotobiotic calves (45–47). Despite its significant economic impact on the livestock industry and status as a pathogen with zoonotic potential, the BNeV life cycle remains largely unknown, mainly due to a lack of a robust and reproducible in vitro cultivation systems. Based on the information that either SAs or HBGAs are used as attachment factors for many caliciviruses, we hypothesized that BNeV might also recognize either SAs or HBGAs as attachment factors for entry and infection. Therefore, the objective of this study was to determine the interaction between BNeV virus-like particles (VLPs) and either SAs or HBGAs using a comprehensive series of BNeV-ligand biochemical assays in

synthetic HBGAs, bovine and human saliva samples, cell cultures, and bovine intestinal tissue sections.

RESULTS

Production and characteristics of BNeV VLPs and hyperimmune antiserum. The VLPs produced from the *Spodoptera frugiperda* ovarian (Sf9) cells infected with the recombinant baculovirus rMA415 had a size of 35-40 nm and appeared empty by electron microscopy (EM) due to the lack of viral nucleic acids (Fig. 1A). Hyperimmune antiserum generated from a rabbit immunized three times with purified VLPs of rMA415 by CsCl density gradient ultracentrifugation detected a specific signal by immunofluorescence in Sf9 cells infected with recombinant baculovirus rMA415 but not in wild-type baculovirus-infected SF9 cells (Fig. 1B). Western blotting with rMA415 hyperimmune antisera detected a 58-kDa protein as expected and consistent with previous reports on other caliciviruses (48, 49).

Carbohydrate moieties act as attachment factors for BNeV. To examine whether carbohydrate moieties are used as attachment factors for BNeV, the carbohydrate moieties were removed from MDBK cells by pretreatment with sodium periodate ($NaIO_4$), which is known to remove the carbohydrate groups without altering cell surface proteins or membranes (50). The binding of Alexa Fluor 594 (AF594)-labeled BNeV VLPs was slightly but significantly increased by pretreating the MDBK cells with 1 mM $NaIO_4$ but was markedly decreased with 10 mM $NaIO_4$ (Fig. 2A). Pretreatment of cells with $NaIO_4$ dose-dependently decreased the binding of the SA-dependent FCV F9 strain, consistent with the high sensitivity of SA to periodate treatment (26). HBGA-dependent VLPs from the HuNoV strain VA387 showed a binding pattern similar to that of BNeV, indicative of binding to neutral sugars (51, 52). However, 1 or 10 mM $NaIO_4$ pretreatment had no inhibitory effect on

146 the binding of the Coxsackievirus B3 (CVB3) strain Nancy, which is known to use decay-
147 accelerating factor (DAF) as a cellular receptor (7, 53).

148 To precisely quantify the inhibitory effect of $NaIO_4$ treatment, radioisotope (RI)-labeled
149 BNeV VLPs and the FCV and CVB3 strains were incubated with the cells pretreated with or
150 without $NaIO_4$ (as mentioned above) and then the degree of binding was measured for each
151 virus by liquid scintillation counting (28). As expected, binding of BNeV VLPs increased to
152 124% with the 1 mM $NaIO_4$ treatment and decreased to 55% with the 10 mM $NaIO_4$
153 treatment in comparison with the mock-treated, VLP-inoculated control (Fig. 2B). The
154 binding of SA-dependent FCV was strongly decreased by both 1 and 10 mM $NaIO_4$ treatment,
155 whereas DAF-dependent CVB3 was not influenced by the treatment (Fig. 2B). Taken
156 together, these results strongly suggest that neutral carbohydrate moieties are involved in the
157 binding of BNeV VLPs to cells.

158 **Terminal SAs are not recognized by BNeV for attachment.** SAs represent a family
159 of sugar molecules that are found mostly at the terminal end of carbohydrates and attach to
160 underlying glycans via α2,3-, α2,6-, or α2,8-linkages (4). Because several caliciviruses,
161 including FCV, PSaV, and MNV, use terminal SAs as attachment factors (5, 26–28), we
162 examined whether SAs act as attachment factors for BNeV using 100 mU *Vibrio cholera*
163 neuraminidase (NA) ml^{-1} which cleaves α2,3-, α2,6- and α2,8-linked SAs (26, 28).
164 Pretreatment of MDBK cells with NA increased the binding of AF594-labeled BNeV VLPs
165 to cells (Fig. 3A), and the binding of RI-labeled BNeV VLPs to cells increased to 123% of
166 the levels observed in the mock-treated cells (Fig. 3B). A similar degree of enhanced binding
167 was observed in the cells treated with HBGA-dependent HuNoV P particles (Fig. 3A).
168 However, SA-dependent FCV showed a marked reduction in cell binding, whereas with

DAF-dependent CVB3 the NA pretreatment had no influence on the degree of binding to cells (Fig. 3). These results support the notion that BNeV does not use terminal SAs as attachment factors and that it uses neutral carbohydrate motifs such as HBGAs instead.

Wide binding spectrum of BNeV VLPs to HBGAs. Using a synthetic HBGA binding assay, we next determined whether HBGAs could be used as attachment factors for BNeV as has been described for other viruses elsewhere (28, 54–56). The BNeV VLPs strongly bound to the immobilized synthetic disaccharide (Fucα1,2Gal) (Fig. 4A), a common motif in HBGAs (57). Moreover, SLe^a, Le^y, Le^x, αGal, H2, H1, SLe^x, H2, and B type immobilized synthetic HBGA oligosaccharides interacted with the BNeV VLPs (ordered from highest to lowest binding degree) (Fig. 4A). The recombinant GST-P particles of the HuNoV strain VA387 and the GST-VP8* proteins of the human rotavirus G11P[25] Dhaka6 and bovine rotavirus G6P[5] WC3 strains bound to their corresponding HBGA types, whereas the supernatant of wild-type baculovirus-infected Sf9 cells and GST had no binding affinity to any HBGA (Fig. 4A). These results indicate that BNeV VLPs recognize a wide spectrum of HBGAs.

HBGA-binding moiety for BNeV VLPs. To identify HBGA-binding epitopes, we examined whether removal of each putative epitope from synthetic HBGAs by pretreatment with α1,2-L-fucosidase, α1,3/4-L-fucosidase, α-galactosidase, or αN-acetylgalactosaminidase was able to decrease the HBGA binding of BNeV VLPs. The results showed that treatment with α1,2-L-fucosidase, which removes the α-1,2-linked-fucose from galactose, significantly decreased the binding of BNeV VLPs to the H type disaccharide, H1 and H2 types, and Le^y carrying α1,2-linked-fucose epitope (Fig. 4B), suggesting that BNeV VLPs recognize the α1,2-linked-fucose as an epitope. In contrast, pretreatment with α1,3/4-L-fucosidase resulted

192 in a significant reduction in the binding of BNeV VLPs to SLe^a, Le^x, SLe^x, and Le^y that all
193 harbor the α1,3/4-linked-fucose epitope (Fig. 4B), confirming binding specificity for this
194 epitope. An almost complete reduction in the binding of BNeV VLPs to Le^y, containing both
195 α1,2- and α1,3/4-linked-fucose epitopes, was observed by combined pretreatment of synthetic
196 Le^y with both enzymes, α1,2-L-fucosidase and α1,3/4-L-fucosidase, supporting the above
197 results that BNeV VLPs recognize both α1,2-linked-fucose- and α1,3/4-linked-fucose.
198 Pretreatment of the Galα3Galβ4GlcNAcβ HBGA with α-galactosidase that cleaves the αGal
199 epitope in Galα3Galβ4GlcNAcβ HBGA had no inhibitory effect on the binding of BNeV
200 VLPs to synthetic Galα3Galβ4GlcNAcβ HBGA (Fig. 4B). However, it significantly reduced
201 the binding of the control GST-VP8* protein of the αGal-dependent bovine rotavirus P[5]
202 WC3 strain to the synthetic Galα3Galβ4GlcNAcβ HBGA (Fig. 5), suggesting that the αGal
203 epitope is not recognized by the BNeV VLPs. Altogether, these results suggest that BNeV
204 VLPs recognize fucose residues in α1,2- and α1,3/4-linkages.

205 **Saliva binding profile of BNeV VLPs.** Because saliva contains mucins carrying
206 HBGAs that are similar to those expressed in the small intestine (2, 8), a saliva-binding assay
207 was performed with the BNeV VLPs, the GST-P particles of the HuNoV strain VA387, and
208 the GST-VP8* proteins of the bovine rotavirus P[5] strain WC3 and human rotavirus P[25]
209 strain Dhaka6 using bovine and human saliva samples, as described elsewhere (55, 56, 58).
210 Prior to determining the binding affinity of BNeV VLPs in the bovine and human saliva
211 samples, the expression levels of each HBGA in the bovine and human saliva samples were
212 examined by enzyme immunoassays as described elsewhere (51, 52, 56). Consistent with
213 previous HBGA phenotyping results for bovine gastrointestinal mucosa (23), the bovine
214 saliva samples contained individually varying levels of A type, H type 2, Le^y and

Galα3Galβ4GlcNAcβ HBGAs and were largely divided into two ABO blood types, H+/A–/B– and H+/A+/B– (Fig. 6A). In addition, the human saliva samples also had variable levels of HBGAs in accordance with ABO and Lewis types (Fig. 6B).

Subsequently, the binding of BNeV VLPs to HBGAs in the bovine and human saliva samples was examined. The BNeV VLPs bound to HBGAs in the bovine saliva samples regardless of the contents of individual HBGAs (Fig. 6A). As a positive control, the recombinant GST-VP8* protein of the bovine rotavirus strain WC3 bound to bovine saliva samples (Fig. 6A). An analogous result was obtained for binding to a range of human saliva samples, regardless of the contents of individual HBGAs (Fig. 6B). As controls, the recombinant GST-VP8* protein of the human rotavirus strain Dhaka6 preferentially bound to human saliva samples rich in A type HBGA (Fig. 7A), whereas the recombinant GST-P particles of the HuNoV strain VA387 showed preferential binding to human saliva samples rich in A and B types of HBGAs (Fig. 7B). All of these data are consistent with the conclusion that a broad range of HBGAs is recognized by BNeV VLPs.

Binding epitopes for BNeV VLPs in the saliva samples. To identify binding epitopes in saliva HBGAs, the effect of pretreating the saliva samples with α1,2-L-fucosidase, α1,3/4-L-fucosidase, α-galactosidase, or αN-acetylgalactosaminidase, either individually or in combination, was examined. Four bovine saliva samples were selected, two of which represented the H+/A+/B- type (samples 2 and 4) and two of which represented the H+/A-/B- type (samples 6 and 10). As each bovine saliva sample expressed different levels of A type, H type 2, Le^y type, and Galα3Galβ4GlcNAcβ, pretreatment with individual enzymes reduced the binding of BNeV to each saliva sample only mildly (Fig. 8A). However, pretreatment of saliva samples with a mixture of α1,2-L-fucosidase and α1,3/4-L-fucosidase resulted in

greater inhibition (Fig. 8A). In addition, pretreatment of the bovine saliva samples with α-galactosidase and αN-acetylgalactosaminidase did not inhibit the binding of BNeV VLPs to any of the selected bovine saliva samples (Fig. 8A), supporting the interpretation that the αGal and GalNAc epitopes are not recognized by the BNeV VLPs. To assess the function of α-galactosidase, the inhibitory effect of α-galactosidase on the binding of the GST-VP8* protein of αGal-dependent bovine rotavirus P[5] strain WC3 to each of the bovine saliva samples was examined. Pretreatment of the bovine saliva samples with α-galactosidase reduced the binding with the control GST-VP8* protein of the αGal-dependent bovine rotavirus P[5] strain WC3 (Fig. 8B).

Each human saliva sample used in this study had different ABH and Lewis antigens depending on the individual (Fig. 6B). Among these samples, six samples representing A (samples 11, 40, and 70) or H (samples 49, 83, and 95) ABH types were selected. Regardless of the ABH types, pretreatment of each saliva sample with a mixture of α1,2-L-fucosidase and α1,3/4-L-fucosidase inhibited the BNeV binding significantly more than that with either α1,2-L-fucosidase or α1,3/4-L-fucosidase individually (Fig. 8C). As expected, pretreatment of the human saliva samples with α-galactosidase or αN-acetylgalactosaminidase had no influence on BNeV binding (Fig. 8C). These results confirmed the wide HBGA-binding spectrum of BNeV VLPs through recognition of α1,2-linked-fucose and α1,3/4-linked-fucose epitopes.

Expression of BNeV-binding HBGA epitopes in cell lines. To further define the BNeV-binding HBGA epitopes, the expression level of the different HBGAs was examined in several cell lines using antibodies specific for each HBGA. The bovine kidney epithelial MDBK, porcine kidney epithelial LLC-PK, canine kidney epithelial MDCK, and feline

kidney CRFK cells solely expressed Galα3Galβ4GlcNAcβ HBGA. Human colorectal adenocarcinoma Caco-2 cells expressed H types 1 and 2, Le^a, Le^x, Le^b, and Le^y HBGAs, whilst human embryonic kidney epithelial 293T cells did not express any of the HBGAs examined. Among these cell lines, MDBK cells were selected to check whether αGal is recognized as an attachment factor for BNeV binding because of sole expression of the αGal-epitope carrying Galα3Galβ4GlcNAcβ HBGA on the cell surface, whereas Caco-2 cells were selected to check whether α1,2-fucose and α1,3/4-fucose epitopes are used as BNeV attachment factors because of expression of multiple HBGAs containing α1,2-fucose and α1,3/4-fucose epitopes on the cell surface HBGAs. The binding of AF594-labeled BNeV VLPs to each cell line was then examined both before and after removal of all of the corresponding HBGAs expressed in each cell line by pretreatment with α1,2-L-fucosidase, α1,3/4-L-fucosidase, α-galactosidase, or αN-acetylgalactosaminidase, either individually or in combination. As expected, removal of αGal from Galα3Galβ4GlcNAcβ HBGA by pretreatment with α-galactosidase had no inhibitory effect on BNeV binding to the MDBK cells, supporting the conclusion that Galα3Galβ4GlcNAcβ HBGA is not used for BNeV attachment (Fig. 9A). To confirm the efficacy of α1,2-L-fucosidase, α1,3/4-L-fucosidase, and α-galactosidase, MDBK and Caco-2 cells were pretreated with each enzyme and then the samples were checked for efficient removal of fucose by using *Ulex Europaeus* agglutinin 1 (UEA-1) that detects fucose residues (59) or an antibody specific to αGal. The pretreatment of cells with α-galactosidase markedly removed αGal residue from MDBK cells, whereas a mixture of α1,2-L-fucosidase and α1,3/4-L-fucosidase significantly removed fucose residues from Caco-2 cells (data not shown). Interestingly, pretreatment of MDBK cells with each fucosidase significantly decreased BNeV VLP binding (Fig. 9A). These effects became more apparent when the cells were pretreated with the mixture (Fig. 9A) even though the cells did

not appear to express fucosylated HBGAs. This suggests that α1,2- and α1,3/4-linked fucose residues not detected by these reagents nonetheless support the binding of BNeV VLPs to MDBK cells. Pretreatment of Caco-2 cells with either α1,2-L-fucosidase or α1,3/4-L-fucosidase also reduced the binding of BNeV VLPs (Fig. 9B). The reduction was much enhanced by pretreatment of the Caco-2 cells with the α1,2-L-fucosidase and α1,3/4-L-fucosidase mixture (Fig. 9B), indicating that BNeV VLP binding involved the α1,2-linked-fucose and α1,3/4-linked-fucose epitopes of HBGAs.

BNeV attachment to CHO cells with expression of H type 2. CHO cells do not express any HBGA on the cell surface due to the lack of α1,2-fucosyltransferase activity and of either the A or B histo-blood group enzymes (60). Whether the above-described binding between BNeV VLPs and HBGAs was similar to that found in parental CHO or transfectant CHO cells, parent and transfectant CHO cells expressing H type 2, A type, B type, or Galα3Galβ4GlcNAcβ HBGAs were examined. After the expression of each target HBGA in parental CHO and transfectant CHO cells as confirmed (Fig. 10A), binding of BNeV VLPs to parental and transfectant CHO cells was analyzed. Compared with parental CHO cells (H–/A–/B–), to which AF594-labeled BNeV VLPs failed to attach, binding of BNeV VLPs was very prominent in CHO cells expressing H type 2 HBGA (H+/A–/B–) (Fig. 10B). It was also detected, albeit less extensively, with A (H+/A+/B–) or B (H+/A–/B+) types (Fig. 10B). As expected, CHO cells expressing Galα3Galβ4GlcNAcβ HBGA had no BNeV VLP binding (Fig. 10B). Taken together, these findings support the overall conclusion that BNeV VLPs have a wide HBGA binding spectrum through specifical reorganization of α1,2- and α1,3/4-linked-fucose residues in the HBGAs.

Determination of BNeV-binding HBGA epitopes in bovine duodenal epithelium. The above results showed that the BNeV VLPs had no binding specificity for terminal SAs on the cultured cell surface. To confirm these results in bovine intestinal tissues, whether removal of terminal or internal parts of cell surface carbohydrate moieties using 1 or 10 mM $NaIO_4$ pretreatment could influence the attachment of BNeV to bovine duodenal epithelium was examined (23). Similar to the aforementioned findings (Fig. 2), abolishment of BNeV binding to the duodenal epithelium was achieved with the 10 mM but not the 1 mM $NaIO_4$ pretreatment (data not shown), suggesting that neutral sugars are also involved in binding to gut tissue. Consistent with this finding, removal of α2,3- and α2,6-linked SAs using NA from *V. cholera* failed to inhibit BNeV VLP binding to gut epithelium (data not shown).

We previously demonstrated that bovine duodenal epithelium expresses A type, H type 2, Le^y, and αGal HBGAs but no other HBGAs by immunohistochemistry (23). Confirming our previous results (23), bovine duodenal sections had two ABO blood types, H+/A–/B–/Ley+/α-Gal+ and H+/A+/B–/Ley+/α-Gal+ (data not shown). These results are consistent with the above findings for the HBGA phenotypes in the saliva samples, with A and O blood types being present in cattle (Fig. 6).

To determine whether BNeV VLPs can recognize HBGAs by binding to α1,2-linked-fucose, α1,3/4-linked-fucose, αGal, or GalNAc epitopes of HBGAs, bovine duodenal paraffin sections showing either O blood type (H+/A–/B–/Le^y+/α-Gal+) or A blood type (H+/A+/B–/Le^y+/α-Gal+) were selected and then pretreated with α1,2-L-fucosidase, α1,3/4-L-fucosidase, α-galactosidase, or αN-acetylgalactosaminidase either individually or in dual combination. As found for the inhibitory effects of HBGA epitope-specific enzymes against BNeV binding to synthetic HBGAs (Fig. 4B), bovine and human saliva samples (Fig. 8), or cultured cells

(Fig. 9), pretreatment of O or A blood type duodenal sections with α-galactosidase or αN-acetylgalactosaminidase produced no inhibitory BNeV binding effects (Fig. 11). However, pretreatment of these duodenal sections with α1,2-L-fucosidase significantly reduced BNeV VLP binding. Pretreatment of duodenal sections with α1,3/4-L-fucosidase partially inhibited the binding of BNeV VLPs to the duodenal epithelium, whilst pretreatment of the duodenal sections with a combination of α1,2-L-fucosidase and α1,3/4-L-fucosidase almost completely abolished the binding of BNeV VLPs to the duodenal epithelium (Fig. 11). Taken together, these results indicate that BNeV VLPs can attach to bovine as well as human glycan compounds on the surface of epithelial cells containing α1,2-linked-fucose and α1,3/4-linked-fucose epitopes, as found in most HBGA epitopes.

DISCUSSION

Viruses must attach to cell surface attachment factor(s) and/or receptor(s) to initiate viral entry and replication (1, 2). Many caliciviruses attach to cell surface carbohydrate moieties, such as HBGAs or SAs (2, 28). Here, we demonstrate that VLPs of the BNeV bind to a wide spectrum of HBGAs present as synthetic neoglycoconjugates, secreted in bovine and human saliva, or expressed by cultured cells and bovine duodenal epithelium. Among HBGA-dependent caliciviruses, some HuNoVs, particularly some GII.4 strains and the recently emerged GII.17 strains, are well known to have a wide binding spectrum of HBGAs in all ABO, Lewis, and secretor/nonsecretor types (2, 58, 61, 62). Generally, it is considered that the multiple binding patterns of HuNoVs to HBGAs could be subdivided into two major binding groups: the A/B or Lewis binding groups (2, 51, 52). The A/B binding group members, including VA387, Norwalk, and MOH strains, are considered to accommodate one or two epitopes of A/B and H HBGAs, i.e., galactose and/or α1,2-linked-fucose. In contrast, the Lewis binding group members, such as the Boxer, VA207, and OIF strains, utilize α1,2-linked-fucose and/or α1,3-linked-fucose epitopes of H and Lewis HBGAs. In the present study, enzymatic removal of α1,2- and α1,3/4-linked-fucoses from the various HBGA backbones reduced BNeV binding to the corresponding synthetic HBGAs and saliva samples. These data indicate that similar to the human Lewis binding group, BNeV VLPs recognize a wide spectrum of HBGAs via binding to their α1,2- and α1,3/4-linked-fucose epitopes (2, 51, 52, 58, 61). As expected, removal of the αGal or GalNAc epitopes had no inhibitory effect on BNeV VLP binding, indicating that BNeV does not use the αGal and GalNAc epitopes as attachment factors. Indeed, it is well known that bovine genogroup III NoV uses the αGal

362 epitope, which is absent from human and pig gut epithelium, suggesting that neither man nor
363 pig could be infected by bovine NoVs (23). However, this remains to be explored.

364 The binding of BNeV VLPs to the bovine duodenal sections was markedly decreased
365 by pretreatment with α1,2-L-fucosidase. This was attributed to the A type/H type 2/Le^y
366 HBGAs from the four types being expressed in bovine duodenal epithelium containing the
367 α1,2-linked-fucose epitope. In addition, there is a slight reduction in BNeV binding to the
368 bovine duodenal sections with the α1,3/4-L-fucosidase pretreatment because the α1,3/4-
369 linked-fucose epitope is present only in Le^y HBGA. However, pretreatment of bovine
370 duodenal sections with α-galactosidase or αN-acetylgalactosaminidase had no inhibitory
371 effect on the binding of BNeV VLPs to the duodenal sections, indicating that the αGal
372 epitope in Galα3Galβ4GlcNAcβ HBGA and the GalNAc epitope in A type HBGA were not
373 be used as attachment epitopes for BNeV binding to the bovine duodenum. These findings
374 also support the conclusion that similar to the human Lewis binding group, BNeV VLPs
375 attach to α1,2- and/or α1,3/4-linked-fucose epitopes in H type 2/Le^y HBGAs expressed in the
376 bovine duodenal epithelium (2, 51, 52, 58, 61).

377 As demonstrated in the present study, BNeV had a wide HBGA binding spectrum
378 through recognition of α1,2-linked-fucose and α1,3/4-linked-fucose epitopes of targeted
379 HBGAs. It should be noted that bovine and human saliva samples have different levels of
380 ABH and Lewis antigens which carry α1,2-linked-fucose and/or α1,3/4-linked-fucose
381 epitopes (23). Therefore, pretreatment of bovine and human saliva samples with a mixture of
382 α1,2-L-fucosidase and α1,3/4-L-fucosidase should have higher inhibitory effects on BNeV
383 binding than that with either α1,2-L-fucosidase or α1,3/4-L-fucosidase individually.

384 Although the synthetic HBGA binding assay showed that the VLPs from BNeV had
385 strong binding to SLe^a HBGA and weak binding to SLe^x HBGA, they were expressed in the
386 bovine small intestinal epithelium or secreted into saliva with the methods used. This means
387 that BNeV does not use SLe^a and SLe^x for entry and infection in cattle. Both SLe^a and SLe^x
388 are expressed at high concentrations in cancer cells such as human colon cancer but only
389 minimally in non-transformed cells, defining their utility as diagnostic cancer markers in
390 human medicine (63). The reason for the binding of BNeV VLPs to SLe^a and SLe^x is the
391 presence of α1,3/4-linked-fucose epitopes (57).

392 SA-containing gangliosides have been identified as attachment factors for murine
393 MNV1, PSaV, and FCV (26–28). Interestingly, recent studies have shown that in addition to
394 HBGAs, SAs can be also used as attachment factor(s) for HuNoVs and Tulane virus, the
395 prototype of the *Recovirus* genus; α2,3- and α2,6-linked SAs, particularly α2,3-linked SA
396 containing GM3, possibly act as attachment factors for HuNoV VA387 (GII.4) and VA115
397 (GI.3) strains, whereas α2,6-linked terminal SAs are likely utilized by Tulane virus (29, 30).
398 In contrast to the reduced binding observed for the Tulane virus (29), in this study, removal
399 of terminal SAs from cell surface carbohydrates by NA and 1 mM $NaIO_4$ had no inhibitory
400 effect on the binding of BNeV VLPs to the cells. Rather, pretreatment with NA and 1 mM
401 $NaIO_4$ increased BNeV VLP binding. This may be due to increased access to fucosylated
402 epitopes following removal of the charged SA motifs. However, pretreatment with 10 mM
403 $NaIO_4$ markedly decreased the BNeV binding to the cells, possibly due to complete removal
404 of HBGAs on the cell surface (23). The lack of inhibition following NA treatment does not
405 rule out the possibility that the internal SAs of gangliosides like GM1a are recognized (64).

406 However, the lack of sensitivity with the 1 mM $NaIO_4$ treatment strongly suggests that this is
407 not the case.

408 In the present study, we demonstrate that BNeV VLPs do not recognize αGal epitope.
409 Additionally, MDBK cells were found to solely express αGal epitope, and not to express
410 fucosylated HBGA with the antibodies used. Therefore, it was anticipated that α1,2- and
411 α1,3/4-linked fucose epitope-dependent BNeV VLPs would not bind the cell surface of
412 MDBK cells. Unexpectedly, however, BNeV VLPs attached to MDBK cells and pretreatment
413 of MDBK cells with these fucosidases inhibited BNeV binding to MDBK cells. The
414 mechanism by which BNeV VLPs bind to MDBK cells remains unclear. Nevertheless, these
415 data suggest that MDBK cells express fucosylated HBGAs, which could not be detected by
416 the antibodies used in this study but could be degraded by fucosidases. The identification of
417 specific fucose-containing epitopes on MDBK cells involved in BNeV binding forms the
418 basis of an ongoing work.

419 Because infection by all viruses begins with the attachment of the virus to the host cells,
420 expression levels of the target receptor for a given virus could be an important factor in
421 determining the viral tropisms, pathogenesis, and host range restriction (6, 66–68). Some
422 NoVs detected in humans and animals have a close genetic relationship and share target
423 receptors, which has raised the questions regarding the possibility of the zoonotic
424 transmission of these viruses (24, 69). For example, porcine NoV strains detected worldwide
425 have close genetic relatedness to HuNoVs (70–77). Moreover, HuNoV strain GII.4-HS66
426 induces diarrhea and intestinal pathology in piglets and calves, respectively (78, 79). Recent
427 studies have shown that primate enteric caliciviruses within the *Recovirus* genus share their
428 HBGA attachment factors with HuNoVs (25, 80). Furthermore, the zoonotic potential of

these viruses has been clearly demonstrated by the high prevalence of neutralizing antibodies (81, 82). In the present study, BNeV utilized HBGAs that are commonly used by HuNoVs and other enteric caliciviruses. This suggests that BNeVs have the potential to infect humans and/or other species. In particular, VLPs from BNeV displayed wide-spectrum binding in human saliva, and human and animal cell lines, further supporting the above hypothesis. It should be noted that bovines express type 2-based HBGAs in their digestive tract but humans have type 1-based structures in their digestive tract. Accordingly, HuNoVs appear to favor the recognition of type 1-based HBGAs (83, 84). BNeVs might be less adapted to human infection, as neither the virus nor its specific antibody have been isolated from and detected in humans.

To demonstrate the direct interspecies transmission of BNeVs, the molecular detection of BNeVs and sequence analysis of resultant amplicons are necessary in stool samples of humans and animals such as pigs, particularly where humans and animals or different animal species live in close physical contact and mixed infections are more common (82). Although robust and reproducible in vitro cultivation systems for BNeVs have not been established, more definitive evidence for the interspecies transmission of BNeVs can be obtained by the inoculation of the BNeV isolates into different species such as human volunteers or piglets. Indirect evidence for interspecies transmission of BNeVs can be provided by the detection of antibodies against BNeVs in serum samples collected from humans and other animals, particularly those living in the above environments (81, 85, 86). Nevertheless, our results stress the need for more in-depth genomic and serological studies of BNeVs in humans and other species.

In conclusion, the present study provides direct evidence that BNeV VLPs attach to H type 2/Le^y/Le^x HBGAs expressed in the bovine digestive tract through their α1,2- and α1,3/4-linked fucose residues. Moreover, the usage of multiple HBGAs by BNeV VLPs and their ability to bind to human saliva suggest that BNeVs may have the potential for zoonotic transmission. More in-depth epidemiological studies using human fecal and serum samples are required to determine the zoonotic potential of BNeVs. Similarly, continued investigations regarding the proteinaceous receptor(s) are necessary for a better understanding of the tropism, pathogenesis, and host range of this important viral genus.

MATERIALS AND METHODS

Cells and viruses. Madin-Darby bovine kidney (MDBK), porcine kidney LLC-PK, and human cervical cancer HeLa cells purchased from American Type Culture Collection (ATCC, USA) were maintained in Eagle's minimum essential medium supplemented with 10% fetal bovine serum (FBS), 100 U/ml penicillin, and 100 µg/ml streptomycin as described elsewhere (7, 87). Madin-Darby canine kidney (MDCK), Crandell-Reese feline kidney (CRFK), human embryonic kidney 293T (HEK293T), and human colorectal adenocarcinoma Caco-2 cells purchased from ATCC were grown in Dulbecco's modified Eagle's medium (DMEM) supplemented with 5% FBS, 100 U/ml penicillin, and 100 µg/ml streptomycin (7, 86). The parental Chinese hamster ovary (CHO) cells that do not express HBGAs (H–/A–/B–) were maintained in RPMI1640 supplemented with 10% FBS, 1% L-glutamine, 100 U/ml penicillin, 100 µg/ml streptomycin, and 10 µg/ml each of adenosine, 2-deoxy-adenosine and thymidine (60). In addition, single-transfectant CHO cells expressing the H antigen (H+/A–/B–) or the αGal antigen, and double-transfectant CHO cells expressing either the A antigen (H+/A+/B–) or the B antigen (H+/A–/B+) were cultured in the conditions described for the parental CHO cells, with addition of 0.2 mg/ml hygromycin and 0.25 mg/ml of G418 (neomycin) to maintain the plasmids expressing the glycosylation enzymes (60). Sf9 cells, purchased from Gibco (Fort Worth, Texas, USA), were cultured at 27°C in SF–900 II SFM media containing 10% FBS, 100 U/ml penicillin, 100 µg/ml streptomycin, lipid medium supplement, and 0.1% pluronic acid solution (Sigma Aldrich, St. Louis, MO, USA). The FCV F9 strain (ATCC) and CVB3 Nancy strain were propagated in CRFK cells and HeLa cells, respectively (26, 88). Cesium chloride (CsCl) density gradient ultracentrifugation was used to purify each mass-cultured strain as described elsewhere (7).

Reagents and antibodies. $NaIO_4$ and NA from Sigma-Aldrich were dissolved in PBS (pH 7.2). Alpha1,2-L-fucosidase from *Corynebacterium* (Takara Bio Inc., Kyoto, Japan), α1,3/4-L-fucosidase from *Streptomyces* (Takara Bio Inc.), α-galactosidase from *Coffea arabica* (Sigma-Aldrich), αN-acetylgalactosaminidase from *Chryseobacterium meningosepticum* (New England BioLabs, Inc., MA, USA), and UEA-1 (Vector Laboratories, Burlingame, CA, USA) were diluted in PBS. AF594 succinimidyl ester, purchased from Molecular Probes (Eugene, OR, USA), was dissolved in DMSO. [^{35}S] methionine/cysteine was purchased from PerkinElmer (Waltham, MA, USA). Biotin-conjugated oligosaccharides including Lewis antigens (Le^a, Le^b, Le^x, and Le^y), H type, type A disaccharide, type B disaccharide, type A trisaccharide, type B trisaccharide, αGal trisaccharide, sialyl-Le^a (SL^a), and SLe^x tetrasaccharides were purchased from GlycoTech (Gaithersburg, MD, USA) (7). The following antibodies were used in this study: hyperimmune sera against BNeV capsid protein, P particles of human NoV VA387 strain, and VP8* protein of human rotavirus Wa strain generated from rabbits by serial inoculation with each target protein as described below, monoclonal antibodies (Mabs) of anti-GST (Santa Cruz Biotechnology), anti-blood group A type antigen (types 1 and 2 chains) (Covance, NJ, USA), anti-blood group H antigen (type 1 chain) (Covance), anti-Le^a antigen (type 1 chain) (Covance), anti-Le^b antigen (type 1 chain) (Covance), anti-Le^x antigen (type 2 chain) (Covance), anti-Le^y antigen (type 2 chain) (Covance), anti-blood group B antigen (Thermo Scientific, MA, USA), anti-H type 2 antigen (Thermo Scientific), anti-αGal epitope antigen (Enzo Life Sciences, Seoul, South Korea), anti-GAPDH Mab (Santa Cruz Biotechnology), anti-rabbit IgG-fluorescence isothiocyanate (FITC)-conjugated antibody (Jackson Immunoresearch Lab, West Grove, PA, USA), biotinylated goat anti-mouse or anti-rabbit antibodies (Dako, Glostrup, Denmark), and anti-mouse IgG-FITC-conjugated antibody (Santa Cruz Biotechnology). Horseradish peroxidase

(HRP)-conjugated streptavidin and HRP-conjugated goat anti-rabbit immunoglobulin G (IgG) and anti-mouse IgG antibodies were obtained from the Jackson Immunoresearch Lab or Dako.

Treatment of cells with chemicals and enzymes. To determine whether BNeVs recognize terminal SAs as attachment factors, the following methods were used as described previously (7). Cells were treated with 1 or 10 mM $NaIO_4$ for 30 min at 4°C or with NA at 100 mU for 1 hr at 37°C in PBS. After the pretreatment, cells were washed three times with PBS. The binding assays were then carried out as described below. Mock and control treatments were performed at the same time.

Expression and purification of BNeV VLPs. BNeV VLPs were generated from a calf diarrhea fecal sample determined positive for BNeV by a PCR based method (38) as described elsewhere (48, 49). Briefly, the complete 2.3 kb capsid region (encoding the VP1-major capsid and VP2-minor capsid regions) of Bo/BNeV/MA415/04/KR was amplified from the above fecal sample by reverse transcription polymerase chain reaction (RT-PCR) with forward (5'-*AAAC*ATGAGTGACAACAAAAGCATCCCAGA-3', nucleotide position 5055 to 5084 of VP1 region) and reverse (5'-TCAAACACTCGTGGTCGAGAACACTGAC-3', nucleotide position 7360 to 7387 of VP2 region) primers designed from the full-length sequence of Newbury agent 1 strain in the Genbank database (accession number NC_007916). The amplicon was ligated into the pCR2.1-TOPO vector (Invitrogen, CA) and then transformed to DH5α competent cells (Enzynomics, Daejeon, Korea). Plasmids were purified using GeneAll Hybrid-Q Plasmid Rapidpre (GeneAll, Seoul, Korea) and the sequence (GenBank accession numbers EF528565, MG009451) was verified using an ABAI system 3700 automated DNA sequencer (Applied Biosystems, Foster City, USA). Using purified plasmid, the full length cDNA copy of capsid

gene was amplified by PCR with forward primer (5'-CACAGGATCCATGAGTGACAACAAAAGCAT-3') containing BamHI restriction site (underlined) and reverse primer (5'-AATCTCGAGTCAAACACTCGTGGTCG-3') containing XhoI restriction site (underlined). After digestion with BamHI and XhoI restriction enzymes, the amplified fragments were subcloned into pFastBac1 baculovirus donor plasmid (ThermoFisher Scientific, Seoul, South Korea). The pFastBac1 donor plasmid was transformed into DH10Bac *Escherichia coli* and its resultant recombinant bacmid DNA was transfected into Sf9 cells using Cellfectin II reagent (Invitrogen; following manufacturer's instruction). BNeV VLPs were expressed in baculovirus recombinant-transformed Sf9 insect cells at 27°C and harvested at 5-7 days post-infection. The cloned recombinant baculovirus generated from pFastBac1 plasmid containing VP1 and VP2 regions of MA415 strain was designed as rMA415 and propagated in Sf9 cells to make master virus stocks. BNeV VLPs were purified using CsCl density gradient ultracentrifugation as described elsewhere (7). The protein concentrations of the VLPs were determined with a BCA protein assay kit (Pierce, IL, USA) according to the manufacturer's instruction. Expression of recombinant capsid protein was validated by electron microscopy, immunofluorescence, and Western blot analyses as described elsewhere (48, 49, 89).

Electron microscopy. VLPs purified from rMA415-infected Sf9 cell culture supernatants by CsCl density gradient ultracentrifugation were stained with 3% phosphotungstic acid (pH 7.0) and examined with an electron microscope (JEM-2000 FXII, JEOL, USA) as described previously (49).

Production of rabbit hyperimmune antiserum. A rabbit hyperimmune antiserum against BNeV VLPs, P particles of human NoV VA387 strain, and VP8* protein of human

552 rotavirus Wa strain was performed as described elsewhere (48, 49). Briefly, two rabbits for
553 each target viral protein were subcutaneously immunized three times with purified BNeV
554 VLPs, P particles of HuNoV, or VP8* protein of rotavirus in complete Freund's adjuvant for
555 the first injection or incomplete Freund's adjuvant for the subsequent infections. The animals
556 were bled 2 weeks after the last booster injection.

557 **Coomassie blue staining and Western blot analysis.** To check the quality and expression of
558 BNeV VLPs, Coomassie blue straining and Western blot analysis were performed as
559 described elsewhere (48, 49, 89). Briefly, the proteins in the supernatant of cells infected with
560 rMA415 or wild-type baculovirus were concentrated by precipitation with 8% polyethylene
561 glycol. The cells infected with rMA415 or wild-type baculovirus were washed three times
562 with cold PBS and lysed using cell extraction buffer containing 10 mM Tris/HCl pH 7.4, 100
563 mM NaCl, 1 mM EDTA, 1 mM EGTA, 1 mM NaF, 20 mM $Na_2P_2O_7$, 2 mM Na_3VO_4, 1%
564 Triton X-100, 10% glycerol, 0.1% SDS, and 0.5% deoxycholate (Invitrogen) for 30 min on
565 ice. Lysates were spun down by centrifugation at 12,000×g for 10 min at 4°C and the samples
566 were analyzed for total protein content with a BCA protein assay kit (Thermo Scientific,
567 Waltham, MA, USA). Samples were resolved by SDS-PAGE and served for Coomassie blue
568 straining or transferred onto nitrocellulose membranes (GE Healthcare Life Sciences). The
569 membranes were blocked for 1 hr at room temperature with Tris-buffered saline containing 5%
570 skimmed milk before they were incubated overnight at 4°C with the primary rabbit
571 polyclonal antibody against BNeV capsid protein. The bound antibody was developed by
572 incubation with a HRP-labeled secondary antibody, and the immunoreactive bands were
573 detected by enhanced chemiluminescence (ECL) (Dogen, Seoul, South Korea) using a
574 Davinch-K Imaging System (Youngwha Scientific Co., Ltd, Seoul, South Korea).

Expression and purification of the GST-P particle and GST-VP8* protein. The GST-P particles of the HuNoV strain VA387 (GII.4) and the GST-VP8* proteins of the human rotavirus P[25] Dhaka6 and bovine rotavirus P[5] WC3 strains were cloned, expressed, and purified as described previously (55, 90). The concentration of the purified NoV P particles and VP8* proteins of the rotavirus strains were determined using a BCA protein assay kit (Pierce, IL, USA) according to the manufacturer's instruction.

AF594 labeling of viruses and VLPs. The FCV F9 and CVB3 Nancy strains, and BNeV VLPs purified by CsCl density gradient ultracentrifugation were labeled with AF594 as described previously (7). Briefly, purified virus particles and VLPs (10 mg at 1 mg ml^{-1}) in 0.1 M sodium bicarbonate buffer (pH 8.3) were labeled with a one-tenth fold-molar concentration of AF594 succinimidyl ester (1 mg at 1 mg ml^{-1} in DMSO). After thorough vortexing for 30 sec, each mixture was incubated for 1 hr at room temperature with continuous stirring. Labeled viruses and VLPs were repurified by CsCl density gradient ultracentrifugation, dialyzed, and stored in 2 μg aliquots at –20°C (91). The concentration of the purified AF594-labeled BNeV VLPs, FCV strain, and CVB3 strain was determined using a BCA protein assay kit (Pierce, IL, USA) according to the manufacturer's instructions. Analysis of SDS-PAGE-separated, AF594-labeled viral particles and VLPs using Coomassie blue staining and Western blotting showed that the label was exclusively coupled to each viral protein.

Immunofluorescence assay. To determine the expression levels of each HBGA antigen on the cell surface, the binding specificity of AF594-labeled BNeV VLPs, FCV strain, and CVB3 strain to various cell lines including transfectant CHO cells, and the expression levels of BNeV VLPs in the Sf9 cells infected with rMA415, the immunofluorescence assay was

performed as described elsewhere (87, 89). Briefly, the confluent cells grown on eight-chamber slides were treated with or without chemicals or enzymes and then fixed with 4% paraformaldehyde in PBS for 1 hr. For detection of the BNeV capsid proteins in the Sf9 cells, mock- or rMA415-infected Sf9 cells grown on microscope cover slides were harvested at 48 and 72 hr post-infection and then fixed with 4% paraformaldehyde in PBS for 1 hr. The cells were then permeabilized by the addition of 0.2% Triton X-100 and washed with PBS containing 0.1% newborn calf serum (PBS-NCS). Mabs specific for each HBGA and a polyclonal antibody against BNeV capsid protein were added to each chamber or cover slides and the slides were incubated at 4°C overnight. The cells were then washed three times with PBS-NCS and FITC-conjugated secondary antibodies were added. After washing, the cells were treated with DAPI solution for the staining of nuclei, mounted using SlowFade Gold antifade reagent (Invitrogen), and then examined under an EZ-C1 confocal microscope using EZ-C1 software (Nikon, Japan). Another set of eight chamber slides treated described above was added with AF594-labeled BNeV VLPs and were used to observe binding as described above. For detecting the BNeV capsid protein in the infected Sf9 cells, mock- or rMA415-infected Sf9 cells were incubated with FITC-conjugated secondary antibody. After washing, the cells were mounted with 60% glycerol in PBS (pH 8.0), and then examined under a fluorescence microscope.

Labeling of viruses and VLPs with [^{35}S] methionine/cysteine. Radioisotope labeling of the FCV F9 and CVB3 Nancy strains with [^{35}S] methionine/cysteine (PerkinElmer) was carried out as described elsewhere (7, 26). Briefly, each individual virus was inoculated at an MOI of 0.1 PFU/cell into confluent monolayers of cells and incubated for 4 hr at 37°C. The medium was replaced with RPMI 1640 lacking methionine and cysteine (Sigma-Aldrich).

Cells were starved for 2 hr and then supplemented with 1 Mbq [^{35}S]methionine/cysteine ml^{-1} (PerkinElmer). At 72 hr post-infection, each labeled virus was purified by CsCl density gradient ultracentrifugation as described (7). BNeV VLPs metabolically radiolabeled with [^{35}S] methionine/cysteine (PerkinElmer) were prepared as described previously with slight modifications (92). Briefly, Sf9 cells were infected with recombinant baculovirus at an MOI of 10 PFU per cell and then incubated for 28 hr. The medium was replaced with non-supplemented Grace's insect medium (Gibco). Cells were starved for 30 min and then 30 μCi [^{35}S]methionine/cysteine ml^{-1} (PerkinElmer) were added. At 4 to 6 hr following radioisotope labeling, the medium was volumetrically replaced with the same amount of Grace's insect medium with Sf-900 II SFM (Gibco). The cultures were harvested when 80% of the cells showed cytopathic effects. Radioisotope-labelled VLPs were purified by CsCl density gradient ultracentrifugation as described (7). The concentration of the purified labeled BNeV VLPs, FCV strain and CVB3 strain was determined using a BCA protein assay kit (Pierce) according to the manufacturer's instruction.

Attachment assay with [^{35}S]methionine/cysteine-labeled VLPs and viruses. Binding of ^{35}[S]methionine/cysteine-labeled BNeV VLPs, and the FCV F9 and CVB3 Nancy strains to each corresponding cell line was performed as described elsewhere (7). Briefly, cells (4 x 10^4/well) were plated into 96-well microtiter plates and then independently incubated with purified [^{35}S]methionine/cysteine-labeled BNeV VLPs, and the FCV and CVB3 strains (50 000 c.p.m.) for 45 min on ice. Cells were washed three times with ice-cold PBS followed by cell lysis with 0.1% sodium dodecyl sulfate and 0.1 M NaOH. Total radioactivity in the cell lysate was determined by liquid scintillation counting.

Synthetic HBGA binding assay. To determine the binding specificity of BNeV VLPs,

644 the GST-VP8* proteins of the human rotavirus P[25] strain Dhaka6 and the GST- P particles
645 of the HuNoV strain VA387 to each HBGA, a synthetic oligosaccharide-based HBGA
646 binding assay was carried out as described elsewhere (7). Briefly, 96-well microtiter plates
647 were coated with 50 μg/ml BNeV VLPs, 10 μg/ml of each GST-tagged-VP8* protein and
648 GST-tagged P particles, the supernatant of wild-type baculovirus-infected Sf9 cell lysate, and
649 GST and then incubated at 4°C overnight. Coated plates were blocked with 5% bovine serum
650 albumin (BSA) for 1 hr at room temperature, and each synthetic oligosaccharide-
651 polyacrylamide (PAA)-biotin conjugate (10 μg/ml) was then added and further incubated at
652 4°C overnight. Bound oligosaccharides were detected using HRP-conjugated streptavidin.
653 The signal intensities were visualized by 3,3',5,5'-tetramethylbenzidine (TMB,
654 Komabiotech), and the absorbance was read at 450 nm wavelength in a plate reader. For each
655 step, the plates were incubated at 37°C for 1 hr and washed five times with PBS containing
656 0.05% Tween 20 (PBS-Tween 20).

657 **Determination of binding epitopes in each synthetic HBGA.** To determine the target
658 HBGA epitopes for the BNeV VLPs, removal of each epitope from the synthetic HBGAs was
659 performed as described previously with slight modifications (23, 93, 94). Briefly, 96-well
660 plates were coated with each of the synthetic HBGAs and incubated at 4°C for 6 hr. The
661 plates were washed thrice with PBS-Tween 20 and blocked with PBS-BSA. After washing
662 three times with PBS, the coated plates were incubated with 100 ul solution containing 20
663 mU/ml of α-1,2-L-fucosidase, 10 μU/ml α-1,3/4-L-fucosidase, 3 mU/ml α-galactosidase or 5
664 mU/ml α-N-acetylgalactosaminidase for 24 hr at 37°C. Thereafter, the plates were washed
665 thrice with PBS and incubated with 50 μg/ml of BNeV VLPs at 4°C for 1 hr. After washing
666 with PBS, the plates were incubated with a hyperimmune serum against BNeV capsid protein.

667 Following this, the plates were washed thrice with PBS and treated with HRP-conjugated
668 goat anti-rabbit IgG. The signals were visualized by TMB followed by absorbance
669 measurement at 450 nm wavelength using a plate reader.

670 **Saliva binding assay.** Saliva samples from 53 human individuals and 8 cows were
671 selected from the Archives of the Saliva Registry of the Laboratory of Veterinary Pathology,
672 College of Veterinary Medicine, Chonnam National University, Gwangju. Before performing
673 the saliva binding assay, the amount of each HBGA content in saliva samples was determined
674 by enzyme immunoassays as described previously (51, 52, 56). Briefly, boiled saliva samples
675 were diluted to 1:20 in PBS and then coated onto microtiter immuno plates (Thermo Fisher
676 Scientific) at 4°C overnight. After blocking with PBS containing 5% BSA at 37°C for 1 hr,
677 Mabs specific to H1, H2, Le^a, Le^b, Le^x, Le^y, type A, type B, and α-Gal HBGAs were added to
678 each well and the plates were incubated for 1 hr at 37°C. After washing, HRP-conjugated
679 goat anti-mouse anti-IgG or IgM were added to each well. After each step, the plates were
680 washed five times with PBS. The color reaction after substrate addition was measured as
681 described above.

682 Binding of the BNeV VLPs, GST-P particles of the HuNoV strain VA387, GST-VP8*
683 proteins of the human rotavirus P[25] strain Dhaka6, and GST-VP8* proteins of the bovine
684 rotavirus P[5] strain WC3 was assessed using the saliva binding assay as described
685 previously with slight modification (51, 52, 56). Briefly, boiled saliva samples were diluted to
686 1:20 and then coated onto 96-well plates at 4°C overnight. After blocking with PBS-BSA at
687 37°C for 1 hr, 50 μg/ml of the BNeV VLPs and 10 μg/ml of each viral protein were added,
688 followed by incubation for 1 hr at 37°C. The bound target proteins were detected using an
689 anti-GST antibody or hyperimmune serum against BNeV capsid protein diluted to 1:1000,

690 followed by addition of HRP-conjugated goat anti-mouse or anti-rabbit IgG antibodies. The
691 signal intensities after addition of substrate were displayed by a TMB kit as described above.

692 **Determination of HBGA binding epitopes in each saliva samples.** To determine the
693 target HBGA epitope for BNeV VLPs, removal of epitopes from selected bovine and human
694 saliva samples was performed as described previously with slight modification (23, 24, 94,
695 95). Briefly, boiled saliva samples were diluted to 1:20 and then coated onto 96-well plates at
696 4°C overnight. The plates were washed thrice with PBS-Tween 20 and then incubated with
697 100 μl solution containing 10 mU/ml of α1,2-L-fucosidase, 10 μU/ml of α1,3/4-L-fucosidase,
698 4 mU/ml of α-galactosidase, or 8 mU/ml of α-N-acetylgalactosaminidase for 48 hr at 37°C.
699 After blocking with PBS-BSA at 37°C for 1 hr, 50 μg/ml BNeV VLPs were added and
700 incubated for 1 hr at 37°C. The bound target proteins were detected using a rabbit
701 hyperimmune serum against BNeV capsid protein diluted to 1:1000, followed by addition of
702 HRP-conjugated goat anti-rabbit IgG antibody. The signal intensities after substrate addition
703 were obtained using a TMB kit as described above.

704 **Tissue samples and immunohistochemical analysis.** Paraffin-embedded bovine small
705 intestinal samples obtained by necropsy from healthy calves were selected from the Archives
706 of the Tissue Registry of the Laboratory of Veterinary Pathology, College of Veterinary
707 Medicine, Chonnam National University, Gwangju. To determine the binding and inhibitory
708 effects of $NaIO_4$ and the enzymes on the binding of BNeV VLPs to bovine small intestinal
709 villous epithelial cells, immunohistochemical analysis was performed as described elsewhere
710 (23, 28). Briefly, tissue sections of 3 um thickness were deparaffinized, rehydrated through a
711 graded ethanol series, and washed in PBS. Thereafter, the sections were treated with 0.3%
712 H_2O_2 in methanol for 20 min to quench endogenous peroxidase, washed three times with PBS,

and blocked with PBS-BSA for 30 min at room temperature in a humid atmosphere to inhibit non-specific binding. To determine the expression of HBGAs, duodenal sections were first treated with the primary Mabs specific for each HBGA and left at 4°C overnight. Washed sections were also treated with or without either $NaIO_4$ at 1 mM or 10 mM in 50 mM sodium acetate buffer (pH 5.0) for 30 min at room temperature, followed by a 10 min incubation with 1% glycine in PBS to remove terminal or internal cell surface carbohydrate moieties, or with enzymes for 18 hr at 37°C for removal of each HBGA epitope or cleaving terminal SAs from epithelial cells. After washing with PBS, the sections were incubated with 10 μg/ml BNeV VLPs, diluted in PBS-BSA, and left at 4°C overnight. They were then washed thrice with PBS-BSA and incubated with a rabbit hyperimmune serum against BNeV capsid protein at 4°C overnight. After washing with PBS, the sections were incubated with biotinylated goat anti-rabbit or anti-mouse secondary antibodies (Dako) followed by peroxidase-conjugated streptavidin (Dako). The reactions were developed with 3,3'-diaminobenzidine tetrahydrochloride (DAB; Vector Laboratories) followed by treatment with Mayer's hematoxylin solution (Merck, Germany) for counterstaining.

Ethics statement. All animals were handled in strict accordance with good animal practices, as described in the NIH Guide for the Care and Use of Laboratory Animals (NIH Publication No. 85-23, 1985, revised 1996). The protocol was approved by the Committee on Ethics of Animal Experiments, CNU (permit number, CNU IACUC-YB-2016-65). The human saliva samples collected with written consent from volunteers were handled in strict accordance with human subjects, as described in the Guidance for the Care and Use of Human Samples of the CNU adhered from the WMA Declaration of Helsinki (Ethical Principles for Medical Research Involving Human Subjects). The protocol was approved by

736 the Committee for Research Ethics Concerning Human Subjects, CNU with permit number
737 (CNU IBR No. 1040198-130807-BR-002-02).

738 **Statistical analyses and software.** Statistical analyses were performed on triplicate
739 experiments using the GraphPad Prism software version 5.03 (GraphPad Software Inc., La
740 Jolla, CA, USA) and a One–Way ANOVA test. *P* values of less than 0.05 were considered to
741 be statistically significant. Figures were generated using Adobe Photoshop CS3 and Prism 5
742 version 5.03.

REFERENCES

1. Grove J, Marsh M. 2011. The cell biology of receptor-mediated virus entry. J Cell Biol 195:1071–1082. https://doi.org/10.1083/jcb.201108131.

2. Tan M, Jiang X. 2014. Histo-blood group antigens: a common niche for norovirus and rotavirus. Expert Rev Mol Med 16:e5. https://doi.org/10.1017/erm.2014.2.

3. Helenius A. 2013. Virus entry and uncoating. p 87–104. In Knipe DM, Howley PM, et al (eds), Fields Virology, 6th ed, Lippincott Williams & Wilkins, Philadelphia, PA.

4. Chen X, Varki A. 2010. Advances in the biology and chemistry of sialic acids. ACS Chem Biol 5:163–176. http://doi.org/10.1021/cb900266r.

5. Neu U, Bauer J, Stehle T. 2011. Viruses and sialic acids: rules of engagement. Curr Opin Struct Biol 21:610–618. http://doi.org/10.1016/j.sbi.2011.08.009.

6. Olofsson S, Bergström T. 2005. Glycoconjugate glycans as viral receptors. Ann Med 37:154–172. http://doi.org/10.1080/07853890510007340.

7. Kim DS, Son KY, Koo KM, Kim JY, Alfajaro MM, Park JG, Hosmillo M, Soliman M, Baek YB, Cho EH, Lee JH, Kang MI, Goodfellow I, Cho KO. 2016a. Porcine sapelovirus uses α2,3-linked sialic acid on GD1a ganglioside as a receptor. J Virol 90:4067–4077. https://doi.org/10.1128/JVI.02449-15.

8. Le Pendu J, Nyström K, Ruvoën-Clouet N. 2014. Host-pathogen co-evolution and glycan interactions. Curr Opin Virol 7:88–94. https://doi.org/10.1016/j.coviro.2014.06.001.

9. Stehle T, Khan ZM. 2014. Rules and exceptions: sialic acid variants and their role in

763 determining viral tropism. J Virol 88:7696–7699. http://doi.org/ 10.1128/JVI.03683-13.
764 10. Green KY. 2007. Caliciviridae: The Noroviruses. p 582-608. In: Knipe DM, Howley PM,
765 et al (eds). Fields Virology, 6th ed, Lippincott Williams & Wilkins, Philadelphia, PA.
766 11. Clarke IN, Estes MK, Green KY, Hansman GS, Knowles NJ, Koopmans MK, Matson
767 DO, Meyers G, Neill JD, Radford A, Smith AW, Studdert MJ, Thiel HJ, Vinjé J. 2012.
768 Caliciviridae. In: Virus Taxonomy: Classification and Nomenclature of Viruses: Ninth
769 Report of the International Committee on Taxonomy of Viruses. Ed: King AMQ, Adams
770 MJ, Carstens EB, Lefkowitz EJ. P 977–986. San Diego, Elsevier.
771 12. Wolf S, Reetz J, Otto P. 2011. Genetic characterization of a novel calicivirus from a
772 chicken. Arch Virol 156:1143–1150. https://doi.org/10.1007/s00705-011-0964-5.
773 13. Wolf S, Reetz J, Hoffmann K, Gründel A, Schwarz BH, Hünel I, Otto P. 2012.
774 Discovery and genetic characterization of novel caliciviruses in German and Dutch
775 poultry. Arch Virol 157:1499–1507. https://doi.org/10.1007/s00705-012-1326-7.
776 14. Day JM, Ballard LL, Duke MV, Schefflerm BE, Zsak L. 2010. Metagenomic analysis of
777 the turkey gut RNA virus community. Virol J 7:313. https://doi.org/10.1186/1743-422X-
778 7-313.
779 15. Liao Q, Wang X, Wang D, Zhang D. 2014. Complete genome sequence of a novel
780 calicivirus from a goose. Arch Virol 159:2529–2531. https://doi.org/10.1007/s00705-
781 014-2083-6.
782 16. Farkas T, Sestak K, Wei C, Jiang X. 2008. Characterization of a rhesus monkey
783 calicivurs representing a new genus of Caliciviridae. J Virol 82:5408–5416.
784 https://doi.org/10.1128/JVI.00070-08.

17. Mikalsen AB, Nilsen P, Frøystad-Saugen M, Lindmo K, Eliassen TM, Rode M, Evensen O. 2014. Characterization of a novel calicivirus causing systemic infection in atlantic salmon (Salmo salar L.): proposal for a new genus of Caliciviridae. PLoS One 9:e107132. http://doi.org/10.1371/journal.pone.0107132.

18. Wang F, Wang M, Dong Y, Zhang B, Zhang D. 2017. Genetic characterization of a novel calicivirus from a goose. Arch Virol 162:2115–2118. http://doi.org/ 10.1007/s00705-017-3302-8.

19. L'Homme Y, Sansregret R, Plante-Fortier E, Lamontagne AM, Ouardani M, Lacroix G, Simard C. 2009. Genomic characterization of swine caliciviruses representing a new genus of Caliciviridae. Virus Genes 39:66–75. https://doi.org/10.1007/s11262-009-0360-3.

20. Ruvoën-Clouet N, Ganière JP, André-Fontaine G, Blanchard D, LePendu J. 2000. Binding of rabbit hemorrhagic disease virus to antigens of the ABH histo-blood group family. J Virol 74:11950–11954. https://doi.org/10.1128/JVI.74.24.11950-11954.2000.

21. Tan M, Jiang X. 2010. Norovirus gastroenteritis, carbohydrate receptors, and animal models. PLoS Pathog 6:e10000983. https://doi.org/10.1371/journal.ppat.1000983.g001.

22. Marionneau S, Ruvoën N, Le Moullac-Vaidye B, Clement M, Cailleau-Thomas A, Ruiz-Palacois G, Huang P, Jing X, Le Pendu J. 2002. Norwalk virus binds to histo-blood group antigens present on gastroduodenal epithelial cells of secretor individuals. Gastroenterology 122:1967–1977. https://doi.org/10.1053/gast.2002.33661.

23. Zakhour M, Ruvoën-Clouet N, Charpilienne A, Langpap B, Poncet D, Peters T, Bovin N, Le Pendu J. 2009. The alphaGal epitope of the histo-blood group antigen family is a

807 ligand for bovine norovirus Newbury2 expected to prevent cross-species transmission.
808 PLoS Pathog 5:e1000504. http://doi.org/10.1371/journal.ppat.1000504.

809 24. Caddy S, Breiman A, Le Pendu J, Goodfellow I. 2014. Genogroup IV and VI canine
810 noroviruses interact with histo-blood group antigens. J Virol 88:10377–10391.
811 https://doi.org/10.1128/JVI.01008-14.

812 25. Farkas T, Cross RW, Hargitt E 3rd, Lerche NW, Morrow AL, Sestak K. 2010. Genetic
813 diversity and histo-blood group antigen interactions of rhesus enteric caliciviruses. J
814 Virol 84:8617–8625. https://doi.org/10.1128/JVI.00630-10.

815 26. Stuart AD, Brown TD. 2007. Alpha2,6-linked sialic acid acts as a receptor for feline
816 calicivirus. J Gen Virol 88:177–186. https://doi.org/10.1099/vir.0.82158-0.

817 27. Taube S, Perry JW, Yetming K, Patel SP, Auble H, Shu L, Nawar HF, Lee CH, Connell
818 TD, Shayman JA, Wobus CE. 2009. Ganglioside-linked terminal sialic acid moieties on
819 murine macrophages function as attachment receptors for Murine noroviruses (MNV). J
820 Virol 83:4092–4101. http://doi.org/ 10.1128/JVI.02245-08.

821 28. Kim DS, Hosmillo M, Alfajaro MM, Kim JY, Park JG, Son KY, Ryu EH, Sorgeloos F,
822 Kwon HJ, Park SJ, et al. 2014. Both α2,3- and 2,6-linked sialic acids on O-linked
823 glycoproteins act as functional receptors for porcine sapovirus. PLoS Pathog
824 10:e1004172. https://doi.org/10.1371/journal.ppat.1004267.

825 29. Han L, Tan M, Xia M, Kitova EN, Jiang X, Klassen JS. 2014. Gangliosides are ligands
826 for human noroviruses. Am Chem Soc 136:12631–12637.
827 https://doi.org/10.1021/ja505272n.

828 30. Tan M, Wei C, Huang P, Fan Q, Quigley C, Xia M, Fang H, Zhang X, Zhong W,
829 Klassen JS, Jiang X. 2015. Tulane virus recognizes sialic acids as cellular receptors. Sci
830 Rep 5:11784. https://doi.org/10.1038/srep11784.

831 31. Haga K, Fujimoto A, Takai-Todaka R, Miki M, Doan YH, Murakami K, Yokoyama M,
832 Murata K, Nakanishi A, Katayama K. 2016. Functional receptor molecules CD300lf and
833 CD300ld within the CD300 family enable murine noroviruses to infect cells. Proc Natl
834 Acad Sci U S A 113:E6248–E6255. https://doi.org/10.1073/pnas.1605575113.

835 32. Orchard RC, Wilen CB, Doench JG, Baldridge MT, McCune BT, Lee YCJ, Lee S, Pruett-
836 Miller SM, Nelson CA, Fremont DH, Virgin HW. 2016. Discovery of a proteinaceous
837 cellular receptor for a norovirus. Science 353:933–936.
838 http://doi.org/10.1126/science.aaf1220.

839 33. Bhella D, Goodfellow IG. 2011. The cryo-electron microscopy structure of feline
840 calicivurs bound to junctional adhesion molecule A at 9-angstrom resolution reveals
841 receptor-induced flexibility and two distinct conformational changes in the capsid protein
842 VP1. J Virol 85:11381–11390. https://doi.org/10.1128/JVI.05621-11.

843 34. Makino A, Shimojima M, Miyazawa T, Kato K, Tohya Y, Akashi H. 2006. Junctional
844 adhesion molecule 1 is a functional receptor for feline calicivirus. J Virol 80:4482–4490.
845 https://doi.org/10.1128/JVI.80.9.4482-4490.2006.

846 35. Sosnovtsev SV, Sandoval-Jaime C, Parra GI, Tin CM, Jones RW, Soden J, Barnes D,
847 Freeth J, Smith AW, Green KY. 2017. Identification of human junctional adhesion
848 molecules 1 as a functional receptor for the Hom-1 calicivirus on human cells. MBio
849 8:e00031–17. http://doi.org/10.1128/mBio.00031-17.

850 36. Ravn V, Dabelsteen E. 2000. Tissue distribution of histo-blood group antigens. APMIS
851 108:1–28.

852 37. Oliver SL, Asobayire E, Dastjerdi AM, Bridger JC. 2006. Genomic characterization of
853 the unclassified bovine enteric virus Newbur agent-1 (Newbury1) endorses a new genus
854 in the family Caliciviridae. Virology 350:240–250.
855 http://doi.org/10.1016/j.virol.2006.02.027.

856 38. Park SI, Jeong C, Park SU, Kim HH, Jeong YJ, Hyun BH, Chun YH, Kang MI, Cho KO.
857 2008. Molecular detection and characterization of unclassified bovine enteric
858 caliciviruses in South Korea. Vet Microbiol 130:371–379.
859 https://doi.org/10.1016/j.vetmic.2008.01.017.

860 39. Alkan F, Karayel İ, Catella C, Bodnar L, Lanave G, Bányai K, Di Martino B, Decaro N,
861 Buonavoglia C, Martella V. 2015. Identification of a bovine enteric calicivirus, Kırklareli
862 virus, distantly related to neboviruses, in calves with enteritis in Turkey. J Clin Microbiol
863 53:3614–3617. http://doi.org/10.1128/JCM.01736-15.

864 40. Kaplon J, Guenau E, Asdrubal P, Pothier P, Ambert-Balay K. 2011. Possible novel
865 Nebovirus genotype in cattle, France. Emerg Infect Dis 17:1120–1123.
866 http://doi.org/10.3201/eid/1706.100038.

867 41. Hassine-Zaafrane M, Kaplon J, Sdiri-Loulizi K, Aouni Z, Pothier P, Aouni M, Ambert-
868 Balay K. 2012. Molecular prevalence of bovine noroviruses and neboviruses detected in
869 central-eastern Tunisia. Arch Virol 157:1599–1604. http://doi.org/10.1007/s00705-012-
870 1344-5.

871 42. Candido M, Alencar AL, Almeida-Queiroz SR, Buzinaro MG, Munin FS, Godoy SH,
872 Livonesi MC, Fernandes AM, Sousa RL. 2016. First detection and molecular
873 characterization of Nebovirus in Brazil. Epidemiol Infect 144:1876–1878.
874 https://doi.org/10.1017/S0950268816000029.

875 43. Di Martino B, Di Profio F, Martella V, Ceci C, Marsilio F. 2011. Evidence for
876 recombination in neboviruses. Vet Microbiol 153:367–372.
877 https://doi.org/10.1016/j.vetmic.2011.05.034.

878 44. Cho YI, Han JI, Wang C, Cooper V, Schwartz K, Engelken T, Yoon KJ. 2013. Case-
879 control study of microbiological etiology associated with calf diarrhea. Vet Microbiol
880 166:375–385. http://doi.org/10.1016/j.vetmic.2013.07.001.

881 45. Bridger JC, Hall GA, Brown JF. 1984. Characterization of a calici-like virus (Newbury
882 agent) found in association with astrovirus in bovine diarrhea. Infect Immun 43:133–138.

883 46. Hall GA, Bridger JC, Brooker BE, Parsons KR, Ormerod E. 1984. Lesions of gnotobiotic
884 calves experimentally infected with a calicivirus-like (Newbury) agent. Vet Pathol
885 21:208–215.

886 47. Smiley JR, Chang KO, Hayes J, Vinje J, Saif LJ. 2002. Characterization of an
887 enteropathogenic bovine calicivirus representing a potentially new calicivirus genus. J
888 Virol 76:10089–10098. http://doi.org/10.1128/JVI.76.20.10089-10098.2002.

889 48. Jiang X, Wang M, Graham DY, Estes MK. 1992. Expression, self-assembly, and
890 antigenicity of the Norwalk virus capsid protein. J Virol 66:6527–6532.

891 49. Han MG, Wang Q, Smiley JR, Chang KO, Saif LJ. 2005. Self-assembly of the

892 recombinant capsid protein of a bovine norovirus (BoNV) into virus-like particles and
893 evaluation of cross-reactivity of BoNV with human noroviruses. J Clin Microbiol
894 43:778–785. http://doi.org/10.1128/JCM.43.2778-785.2005.
895 50. Woodward MP, Young WW Jr, Bloodgood RA. 1985. Detection of monoclonal
896 antibodies specific for carbohydrate epitopes using periodate oxidation. J Immunol
897 Methods 78:143–153.

898 51. Huang P, Farkas T, Marionneau S, Zhong W, Ruvoen-Clouet N, Morrow AL, Altaye M,
899 Pickering LK, Newbur DS, LePendu J, Jiang J. 2003. Noroviruses bind to human ABO,
900 Lewis, and secretor histo-blood group antigens: identification of 4 distinct strain-specific
901 patterns. J Infect Dis 188:19–31. http://doi.org/10.1086/375742.

902 52. Huang P, Farkas T, Zhong W, Than M, Thornton S, Morrow AL, and Jiang X. 2005.
903 Norovirus and histo-blood group antigens: demonstration of a wide spectrum of strain
904 specificities and classification of two major binding groups among multiple binding
905 patterns. J Virol 79:6714–6722. http://doi.org/10.1128/JVI.79.11.6714-6722.2005.

906 53. Hafenstein S, Bowman VD, Chipman PR, Kelly CMB, Lin F, Medof ME, Rossmann
907 MG. 2007. Interaction of decay-accelerating factor with coxsackievirus B3. J Virol
908 81:12927–12935. http://doi.org/10.1128/JVI.00931-07.

909 54. Hu L, Crawford SE, Czako R, Cortes-Penfield NW, Smith DF, Le Pendu J, Estes MK,
910 Prasad BV. 2012. Cell attachment protein VP8* of a human rotavirus specifically
911 interacts with A-type histo-blood group antigen. Nature 485:256–259.
912 http://doi.org/10.1038/nature10996.

913 55. Huang P, Xia M, Tan M, Zhong W, Wei C, Wang L, Morrow A, Jiang X. 2012. Spike
914 protein VP8* of human rotavirus recognizes histo-blood group antigens in a type-
915 specific manner. J Virol 86:4833–4843. http://doi.org/10.1128/JVI.05507-11.

916 56. Liu Y, Huang P, Tan M, Liu M, Liu Y, Biesiada J, Meller J, Castello AA, Jiang B, Jiang
917 X. 2012. Rotavirus VP8*: Phylogeny, host range, and interaction with histo-blood group
918 antigens J Virol 86:9899–9910. https://doi.org/10.1128/JVI.00979-12.

919 57. Marionneau S, Cailleau-Thomas A, Rocher J, Moullac-Vaidye B L, Ruvoën N, Clément
920 M, Pendu J L. 2001. ABH and Lewis histo-blood group antigens, a model for the
921 meaning of oligosaccharide diversity in the face of a changing world. Biochimie 83:565–
922 573.

923 58. Zhang XF, Huang Q, Long Y, Jiang X, Zhang T, Tan M, Zhang QL, Huang ZY, Li YH,
924 Ding YQ, Hu GF, Tang S, Dai YC. 2015. An outbreak caused by GII.17 norovirus with a
925 wide spectrum of HBGA-associated susceptibility. Sci Rep 5:1–10.
926 https://doi.org/10.1038/srep17687.

927 59. Thomas CJ, Surolia A. 2000. Mode of molecular recognition of L-fucose by fucose-
928 binding legume lectins. Biochem Biophys Res Commu 268:262–267.
929 http://doi.org/10.1006/bbrc.2000.2.2110.

930 60. Guillon P, Clément M, Sébille V, Rivain JG, Chou CF, Ruvoën-Clouet N, Le Pendu J.
931 2008. Inhibition of the interaction between the SARS-CoV spike protein and its cellular
932 receptor by anti-histo-blood group antibodies. Glycobiology 18:1085–1093
933 http://doi.org/10.1093/glycob/cwn093.

61. Chan MC, Lee N, Hung TN, Kwok K, Cheung K, Tin EK, Lai RW, Nelson EA, Leung TF, Chan PK. 2015. Rapid emergence and predominance of a broadly recognizing and fast-evolving norovirus GII.17 variant in late 2014. Nat Commun 6:10061. https://doi.org/10.1038/ncomms10061.

62. de Rougemont A, Ruvoen-Clouet N, Simon B, Estienney M, Elie-Caille C, Aho S, Pothier P, Le Pendu J, Boireau W, Belliot G. 2011. Qualitative and quantitative analysis of the binding of GII.4 norovirus variants onto human blood group antigens. J Virol 85:4057–4070. https://doi.org/10.1128/JVI.02077-10.

63. Trinchera M, Aronica A, Dall'Olio F. 2017. Selectin ligands sialyl-Lewis a and sialyl-Lewis x in gastrointestinal cancers. Biology 6:E16. http://doi.org/10.3390/biology6010016.

64. Haselhorst T, Fleming FE, Dyason JC, Hartnell RD, Yu X, Holloway G, Santegoest K, Kiefel MJ, Blanchard H, Coulson BS, von Itzstein M. 2009. Sialic acid dependence in rotavirus host cell invasion. Nat Chem Biol 5:91–93. http://doi.org/10.1038/nchembio.134.

65. Wiese TJ, Dunlap JA, Yorek MA. 1994. L-fucose is accumulated via a specific transport system in eukaryotic cells. J Biol Chem 269:22705–22711.

66. de Graaf M, Fouchier RA. 2014. Role of receptor binding specificity in influenza A virus transmission and pathogenesis. EMBO J 33:823–841. https://doi.org/10.1002/embj.201387442.

67. Morizono K, Chen ISY. 2011. Receptors and tropisms of envelope viruses. Curr Opin Virol 1:13–18. http://doi.org/10.1016/j.coviro.2011.05.001.

956 68. Schneider-Schaulies J. 2000. Cellular receptors for viruses: links to tropism and
957 pathogenesis. J Gen Virol 81:1413–1429.

958 69. Bank-Wolf BR, König M, Thiel HJ. 2010. Zoonotic aspects of infections with
959 noroviruses and sapoviruses. Vet Microbiol 140:204–212.
960 http://doi.org/10.1016/j.vetmic.2009.08.021.

961 70. Chao DY, Wei JY, Chang WF, Wang J, Wang LC. 2012. Detection of multiple
962 genotypes of calicivirus infection in asymptomatic swine in Taiwan. Zoonoses Public
963 Health 59:434–444. https://doi.org/10.1111/j.1863-2378.2012.01483.x.

964 71. Di Bartolo I. Tofani S, angenoni G, Ponterio E, Ostanello F, Ruggeri FM. 2014.
965 Detection and characterization of porcine caliciviruses in Italy. Arch Virol 159:2479–
966 2484. http://doi.org/10.1007/s00705-014-2076-5.

967 72. Keum HO, Moon HJ, Park SJ, Kim HK, Rho SM, Park BK. 2009. Porcine noroviruses
968 and sapoviruses on Korean swine farms. Arch Virol 154:1765-1774. J Virol 87:7255–
969 7264. http://doi.org/10.1007/s00705-009-0501-y.

970 73. L'Homme Y, Sansregret R, Plante-Fortier E, Lamontagne AM, Lacroix G, Ouardani M,
971 Deschamps J, Simard G, Simard C. 2009b. Genetic diversity of porcine Norovirus and
972 Sapovirus: Canada, 2005-2007. Arch Virol 154:581–593. https://doi.org/10.1007/s00705-
973 009-0344-6.

974 74. Mattison K, Shukla A, Cook A, Pollari F, Friendship R, Kelton D, Bidawid S, Farber JM.
975 2007. Human noroviruses in swine and cattle. Emerg Infect Dis 13:1184–1188.
976 https://doi.org/10.3201/eid1308.070005.

977 75. Reuter G, Biró H, Szucs G. 2007. Enteric caliciviruses in domestic pigs in Hungary.
978 Arch Virol 152:611–614. http://doi.org/10.1007/s00705-006-0887-8.

979 76. Sugieda M, Nagoka H, Kakishima Y, Ohshita T, Nakamura S, Nakajima S. 1998.
980 Detection of Norwalk-like virus genes in the caecum contents of pigs. Arch Virol
981 143:1215–1221.

982 77. Wang QH, Han MG, Cheetham S, Souza M, Funk JA, Saif LJ. 2005. Porcine noroviruses
983 related to human noroviruses. Emerg Infect Dis 11:1874–1881. http://doi.org/
984 10.3201/eid1112.050485.

985 78. Cheetham S, Souza M, Meulia T, Grimes S, Han MG, Saif LJ. 2006. Pathogenesis of a
986 genogroup II human norovirus in gnotobiotic pigs. J Virol 80:10372–10381.
987 http://doi.org/10.1128/JVI.00809-06.

988 79. Souza M, Azevedo MS, Jung K, Cheetham S, Saif LJ. 2008. Pathogenesis and immune
989 responses in gnotobiotic calves after infection with the genogroup II.4-HS66 strain of
990 human norovirus. J Virol 82:1777–1786. http://doi.org/10.1128/JVI.01347-07.

991 80. Farkas T. 2015. Rhesus enteric calicivirus surrogate model for human norovirus
992 gastroenteritis. J Gen Virol 96:1504–1514. https://doi.org/10.1099/jgv.0.000020.

993 81. Farkas T, Lun CWP. 2014. Prevalence of recovirus-neutralizing antibodies in human
994 serum samples. J Clin Microbiol 52:3088–3090. https://doi.org/10.1128/JCM.01187-14.

995 82. Smits SL, Rahman M, Schapendonk CM, van Leeuwen M, Faruque AS, Haagmans BL,
996 Endtz HP, Osterhaus AD. 2012. Calicivirus form novel Recovirus genogroup in human
997 diarrhea, Bangladesh. Emerg Infect Dis 18:1192–1195.
998 http://doi.org/10.3201/eid1807.120344.

999 83. Fiege B, Leuthold M, Parra F, Dalton KP, Meloncelli PJ, Lowary TL, Peters T. 2017.
1000 Epitope mapping of histo blood group antigens bound to norovirus VLPs using STD
1001 NMR experiments reveals find details of molecular recognition. Glycoconj J 34:679–689.
1002 https://doi.org/10.1007/s10719-017-9792-5.

1003 84. Nasir W, Frank M, Kunze A, Bally M, Parra F, Nyholm PG, Höök F, Larson G. 2017.
1004 Histo-blood group antigen presentation is critical for binding of norovirus VLP to
1005 glycosphingolipids in model membranes. ACS Chem Biol 12:1288–1296.
1006 http://doi.org/10.1021/acschembio.7b00152.

1007 85. Mesquita JR, Costantini VP, Cannon JL, Lin SC, Nascimento MS, Vinje J. 2013.
1008 Presence of antibodies against genogroup VI norovirus in humans. Virol J 10:176.
1009 http://doi.org/10.1186/1743-422X-10-176.

1010 86. Widdowson M, Rockx B, Schepp R, van der Poel WHM, Vinje J, van Duynhoven YT,
1011 Koopmans MP. 2005. Detection of serum antibodies to bovine norovirus in veterinarians
1012 and the general population in the Netherlands. J Med Virol 76:119–128.
1013 http://doi.org/10.1002/jmv.20333.

1014 87. Kim DS, Kang MI, Son KY, Bak GY, Park JG, Hosmillo M, Seo JY, Kim JY, Alfajaro
1015 MM, Soliman M, Baek YB, Cho EH, Lee JH, Kwon J, Choi JS, Goodfellow I, Cho KO.
1016 2016b. Pathogenesis of Korean Sapelovirus A in piglets and chicks. J Gen Virol
1017 97:2566–2574. https://doi.org/10.1099/jgv.0.000571.

1018 88. Shafren DR, Williams DT, Barry RD. 1997. A decay-accelerating factor-binding strain of
1019 coxsackievirus B3 requires the coxsackievirus-adenovirus receptor protein to mediate
1020 lytic infection of rhabdomyosarcoma cells. J Virol 71:9844–9848.

1021 http://doi.org/10.1128/JVI.01827-10.

1022 89. Senger T, Schadlich L, Gissmann L, Muller M. 2009. Enhanced papillomavirus-like
1023 particle production in insect cells. Virology 388:344–353.
1024 https://doi.org/10.1016/j.virol.2009.04.004.

1025 90. Tan M, Zhong W, Song D, Thornton S, Jiang X. 2004. E. coli-expressed recombinant
1026 norovirus capsid proteins maintain authentic antigenicity and receptor binding capability.
1027 J Med Virol 74:641–649.

1028 91. Pelkmans L, Helenius A. 2003. Insider information: what viruses tell us about
1029 endocytosis. Curr Opin Microbiol 15:414–422. https://doi.org/10.1016/s0955-0674
1030 (03)00081-4.

1031 92. White LJ, Ball JM, Hardy ME, Tanaka TN, Kitamoto N, Estes MK. 1996. Attachment
1032 and entry of recombinant Norwalk virus capsids to cultured human and animal cell lines.
1033 J Virol 70:6589–6597.

1034 93. Azuma Y, Sakanashi M, Matsumono K. 2001. The effect of α2,6-linked sialic acid on
1035 anti-IgM antibody-induced apoptosis in Ramos cells. Glycoconjugate J 18:419–424.

1036 94. Seidman D, Hebert KS, Truchan HK, Miller DP, Tegels BK, Marconi RT, Carlyon JA.
1037 2015. Essential domains of *Anaplasma phagocytophilum* invasins utilized to infect
1038 mammalian host cells. PLoS Pathog 11:e1004669.
1039 http://doi.org/10.1371/journal.ppat.1004669.

1040 95. Hebert KS, Seidman D, Oki AT, Izac J, Emani S, Jr. Oliver LD, Miller DP, Tegels BK,
1041 Kannagi R, Marconi RT, Carlyon JA. 2017. *Anaplasma marginale* outer membrane
1042 protein A is an adhesion that recognizes sialylated and fucosylated glycans and

1043 functionally depends on an essential binding domain. Infect Immun 85:e00968–16.
1044 http://doi.org/10.1128/IAI.00968-16.

ACKNOWLEDGEMENT

We would like to thank Ulrich Desselberger (Department of Medicine, University of Cambridge, UK) for insightful comments on this manuscript. KCHO was supported by a grant (2017R1A2B3002971) from the Basic Science Research Program through the National Research Foundation of Korea (NRF) that is funded by the Ministry of Science, ICT and Future Planning, Republic of Korea. JLP was supported by the ARMINA project, a grant from the Région des Pays de la Loire, France.

Figure Legends

FIG 1 Electron micrograph of BNeV VLPs from and detection of BNeV capsid protein in rMA415-infected insect cells by immunofluorescence assay. (A) The rMA415 VLPs were purified by CsCl gradients from the cell culture supernatants of rMA415-infected Sf9 cells and visualized by negative staining with 3% phosphotungstic acid (pH 7.0). The right panel is a magnification of the left panel. (B) Sf9 cells were mock-infected (left panel) or infected with rMA415. After 48 (middle panel) and 72 hr post-infection (right panel), cells were immunostained using the rabbit hyperimmue serum against BNeV VLP and FITC-conjugated goat anti-rabbit IgG antibody. The scale bars for left and right panels correspond to 50 μm.

FIG 2 Binding of BNeV VLPs to cell surface carbohydrate. MDBK, CRFK, Caco-2 and HeLa cells were pretreated with 1 mM or 10 mM $NaIO_4$ to remove the carbohydrate moieties. (A) Cells were incubated with the AF594-labeled BNeV VLPs, P particles of human NoV VA387 strain, FCV F9 strain, and CVB3 Nancy strain at 10 μg/ml and then examined by confocal microscopy. (B) The [^{35}S]Methionine/Cysteine-labeled BNeV VLPs, control FCV F9 strain, or CVB3 Nancy strain (50 000 c.p.m.) were bound to MDBK, CRFK, or HeLa cells following pretreatment with or without $NaIO_4$. Binding was quantified by liquid scintillation counting. All experiments were performed three independent times, and Figure A shows one representative set of results. The scale bars in Figure A correspond to 10 μm. Error bars indicate SD from triplicate samples. *$p < 0.05$, **$p < 0.005$.

FIG 3 Lack of BNeV VLP binding to cell surface terminal sialic acids (SAs). MDBK, CRFK, Caco-2, and HeLa cells were pretreated with 100 mU *V. cholerae* neuraminidase (NA) ml^{-1} to remove α2,3-, α2,6- and α2,8-linked SAs from the carbohydrate moieties. (A) The AF594-

1074 labeled BNeV VLPs, FCV F9 strain, P particles of human NoV VA387 strain, and CVB3
1075 Nancy strain were added to the cells at 10 μg/ml, and then examined by confocal microscopy.
1076 (B) The [^{35}S]Methionine/Cysteine-labeled BNeV VLPs, control FCV F9 strain, or CVB3
1077 Nancy strain (50 000 c.p.m.) were bound to MDBK, CRFK, Caco-,2 or HeLa cells after
1078 being pretreated with or without NA. Binding was measured by liquid scintillation counting.
1079 All experiments were performed three independent times, and Figure A shows one
1080 representative set of results. The scale bars correspond to 10 μm. Error bars indicate SD
1081 determined from triplicate samples. *$p < 0.05$, **$p < 0.005$.

1082 **FIG 4** Binding and blocking of BNeV VLPs to synthetic HBGAs. (A) Ninety-six-well plates
1083 were coated with 50 μg/ml BNeV VLPs, GST-tagged-VP8* protein and GST-tagged P
1084 particles (10 μg/ml), supernatant of wild-type baculovirus-infected Sf9 cells lysate and GST
1085 and then incubated with each of the synthetic HBGAs (10 μg/ml). The binding of each
1086 HBGA to target viral proteins and the control was determined by addition of horseradish
1087 peroxidase-conjugated streptavidin as described in the Materials and Methods section. (B)
1088 Alpha1,2-linked-fucose, α1,3/4-linked-fucose, αGal, and GalNAc epitopes were removed
1089 from each of synthetic HBGAs coted in each well using the corresponding enzyme. After
1090 incubation of BNeV VLPs at 50 μg/ml, the binding of BNeV VLPs was determined using
1091 hyperimmune serum against BNeV capsid protein, followed by addition of horseradish
1092 peroxidase-conjugated goat anti-rabbit IgG antibody. The signal intensities for Figures A and
1093 B graphs were visualized using the TMB at 450 nm in three independent experiments. Error
1094 bars indicate SD from triplicate samples.

1095 **FIG 5** Blocking of the binding of GST-VP8* protein of bovine rotavirus P[5] WC3 strain to
1096 synthetic HBGAs. Alpha1,2-linked-fucose, α1,3/4-linked-fucose, αGal, and GalNAc epitopes

were removed from each synthetic HBGA using the corresponding enzyme. Reduction in binding specificity to the VP8* protein of the bovine rotavirus P[5] WC3 strain was determined using the HBGA-binding assay. The signal intensities were visualized by TMB at 450 nm in three independent experiments. Error bars indicate SD from triplicate samples.

FIG 6 Binding between BNeV VLPs and saliva samples. (A) Expression levels of each HBGA in eight boiled bovine saliva samples coated onto 96-well plates were determined using mouse monoclonal antibodies specific for each HBGA, followed by the addition of horseradish peroxidase-conjugated goat anti-mouse IgG and IgM antibody. After characterization of HBGA expression levels in each saliva sample, binding specificity of BNeV VLPs and VP8* protein of bovine rotavirus strain WC3 to each saliva sample was determined by saliva-binding assay. The horizontal red line represents the OD values for BNeV VLP binding for each saliva sample. The horizontal blue line represents the OD values for VP8* protein of bovine rotavirus WC3 strain. (B) Expression levels of each HBGA in 53 human saliva samples were determined as described above. Binding specificity of BNeV VLPs to each saliva sample was determined by saliva-binding assay as described in the Materials and Methods section. The horizontal red line represents the OD values for BNeV VLP binding for each saliva sample. Binding of BNeV VLPs to each sample was visualized using TMB and measured at 450 nm in three independent experiments. Error bars indicate SD from triplicate samples.

FIG 7 Binding of the rotavirus VP8* protein and human NoV P particles to human saliva samples. (A) The GST-VP8* protein of the human rotavirus P[25] Dhaka6 strain was tested as a positive control for binding to a panel of saliva samples from 53 human individuals. Binding results for the individual saliva samples were sorted by A type and non-A type

HBGA signals for the individual saliva samples. (B) The GST-P particles of the human norovirus strain VA387 (GII.4) were tested as a positive control for binding to a panel of saliva samples from 53 human individuals. The binding of P particles was plotted by sorting of the A and B type signals from individual saliva samples. Binding of BNeV VLPs to each sample was visualized using TMB and measured at 450 nm in three independent experiments. Error bars indicate SD from triplicate samples.

FIG 8 Blocking of binding of BNeV VLPs and VP8* protein of bovine P[5] strain WC3 to bovine and human saliva samples. (A) Four selected bovine saliva samples expressing either A type (H+/A+/B–) or H type (H+/A–/B–) were coated onto 96-well plates prior to removal of α1,2-linked-fucose, α1,3/4-linked-fucose, αGal, and GalNAc epitopes from HBGAs by pretreatment with a single specific enzyme or a combination of enzymes. A reduction in the HBGA binding specificity of BNeV VLPs to each bovine saliva sample was determined by saliva-binding assay using hyperimmune serum against BNeV capsid protein as described in the Materials and Methods section. (B) The GST-VP8* protein of the bovine rotavirus P[5] WC3 strain was used as a positive control. Four bovine saliva samples expressing either A-type (H+/A+/B–) or H-type (H+/A–/B–) HBGAs were used to remove α1,2-linked-fucose, α1,3/4-linked-fucose, αGal, and GalNAc epitopes from HBGAs in the saliva samples by individual or combinatorial enzyme pretreatment. A reduction in the HBGA binding specificity of VP8* protein of bovine rotavirus strain WC3 was determined by a saliva-binding assay using hyperimmune serum against VP8* protein. (C) Six human saliva samples expressing either A type (H+/A+/B–) or H type (H+/A–/B–) were used to remove α1,2-linked-fucose, α1,3/4-linked-fucose, αGal, and GalNAc epitopes from HBGAs in the saliva samples by pretreatment with each specific enzyme individually or in various combinations.

Reduction in the HBGA binding specificity of BNeV VLPs was determined by a saliva-binding assay using hyperimmune serum against BNeV capsid protein as described in the Materials and Methods section. Blocking of BNeV VLPs to each sample was visualized using TMB and measured at 450 nm in three independent experiments. Error bars indicate SD from triplicate samples.

FIG 9 Determination of BNeV-binding HBGA epitopes in MDBK and Caco-2 cells. (A) Bovine kidney epithelial MDBK cells were pretreated with or without each specific enzyme (α1,2-L-fucosidase, α1,3/4-L-fucosidase, α-galactosidase, or αN-acetylgalactosaminidase) individually or in various combinations as indicated, mock-treated or applied with 10 μg/ml AF594-labeled BNeV VLPs, and then examined by confocal microscopy. (B) To remove α1,2-linked-fucose, α1,3/4-linked-fucose, αGal, GalNAc epitopes, or α1,2- and α1,3/4-linked-fucoses together, human colorectal adenocarcinoma Caco-2 cells were pretreated with or without each individual enzyme or combinations of the enzymes as indicated, mock-treated or applied with AF594-labeled BNeV VLPs at 10 μg/ml, and then examined by confocal microscopy. All experiments were performed three independent times, and Figures A-C show one representative set of results. The scale bars correspond to 50 μm.

FIG 10 Binding of BNeV VLPs to parent and transfectant CHO cells stably expressing HBGAs. (A) The expression of target HBGA in the parental CHO (H–/A–/B–) cells, single-transfectant CHO cells expressing the H antigen (H+/A–/B–) or the αGal antigen (H–/A–/B–/αGal+), and double-transfectant CHO cells expressing either the A antigen (H+/A+/B–) or the B antigen (H+/A–/B+) were determined using antibodies specific for each target HBGA via confocal microscopy. (B) The parental and transfectant CHO cells stably expressing target HBGA were applied with AF594-labeld BNeV VLPs (10 μg/ml), and then examined

by confocal microscopy. All experiments were performed three independent times, and each panel shows one representative set of results. The scale bars correspond to 50 μm.

FIG 11 Binding inhibition of BNeV VLPs to bovine small intestinal epithelium by HBGA epitope-specific enzymes. (A) H+/A+/B–/Le^y+/α-Gal+ tissue sections and (B) H+/A–/B–/Le^y+/α-Gal+ tissue sections were pretreated with enzymes specifically cleaving α-1,2-linked-fucose, α-1,3/4-linked-fucose, αGal, or GalNAc prior to incubation with BNeV VLPs at 10 μg/ml. Binding of BNeV VLPs was then detected using a rabbit hyperimmune serum against BNeV capsid protein. The experiment was performed in triplicate and one representative set of results is shown. The scale bars correspond to 200 μm.

A

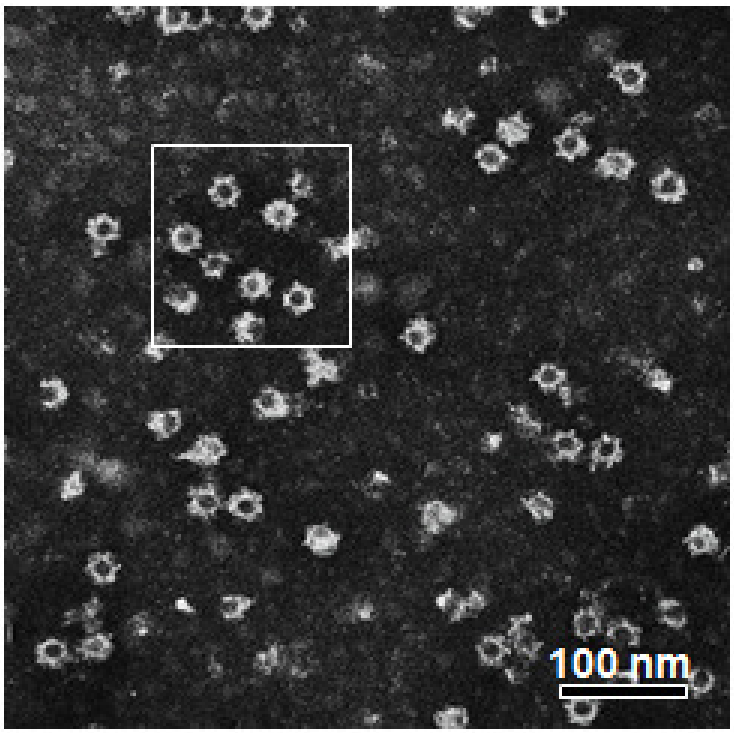

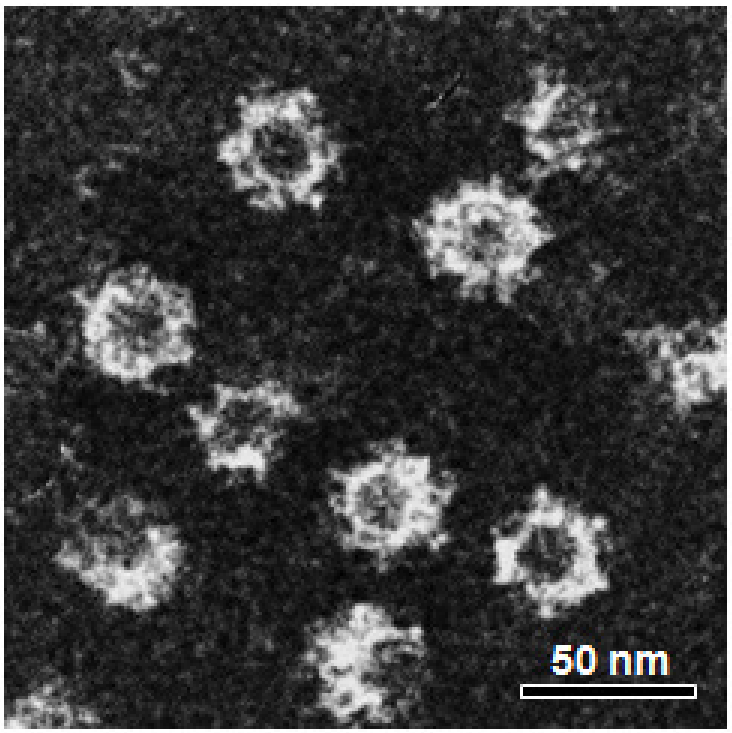

B

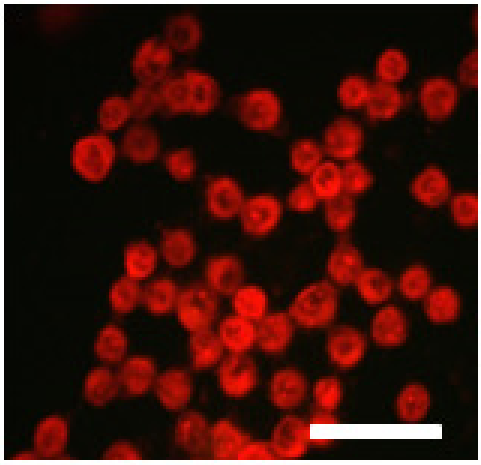

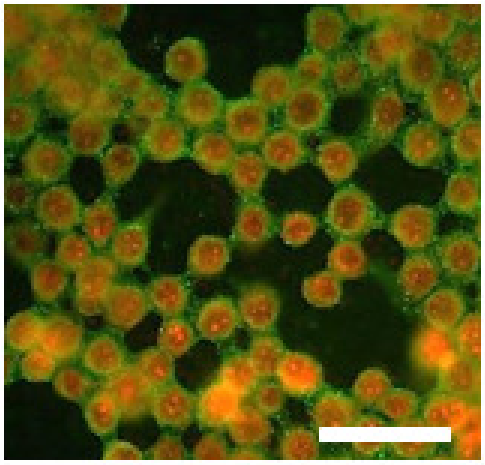

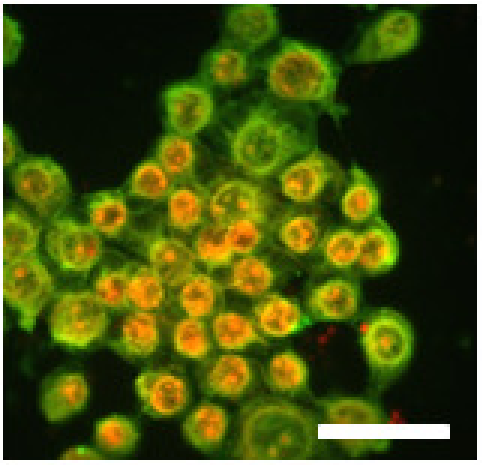

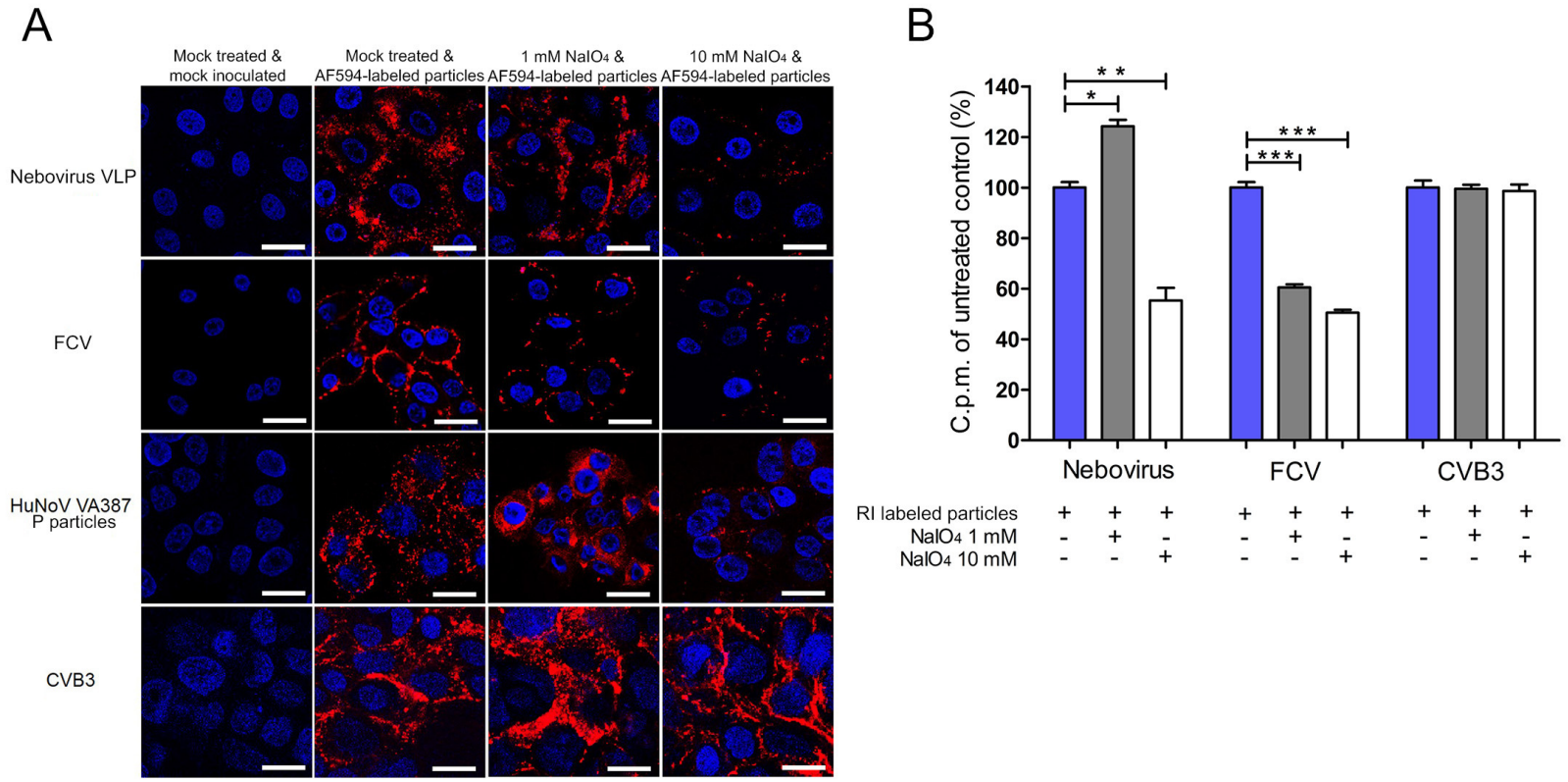
A
Mock treated & mock inoculated
Mock treated & AF594-labeled particles
1 mM NaIO4 & AF594-labeled particles
10 mM NaIO4 & AF594-labeled particles
Nebovirus VLP
FCV
HuNoV VA387 P particles
CVB3
B
C.p.m. of untreated control (%)
140
120
100
80
60
40
20
0
* *
*
***
***
Nebovirus
FCV
CVB3
RI labeled particles + + + + + + + + +
NaIO4 1 mM - + - - + - - + -
NaIO4 10 mM - - + - - + - - +

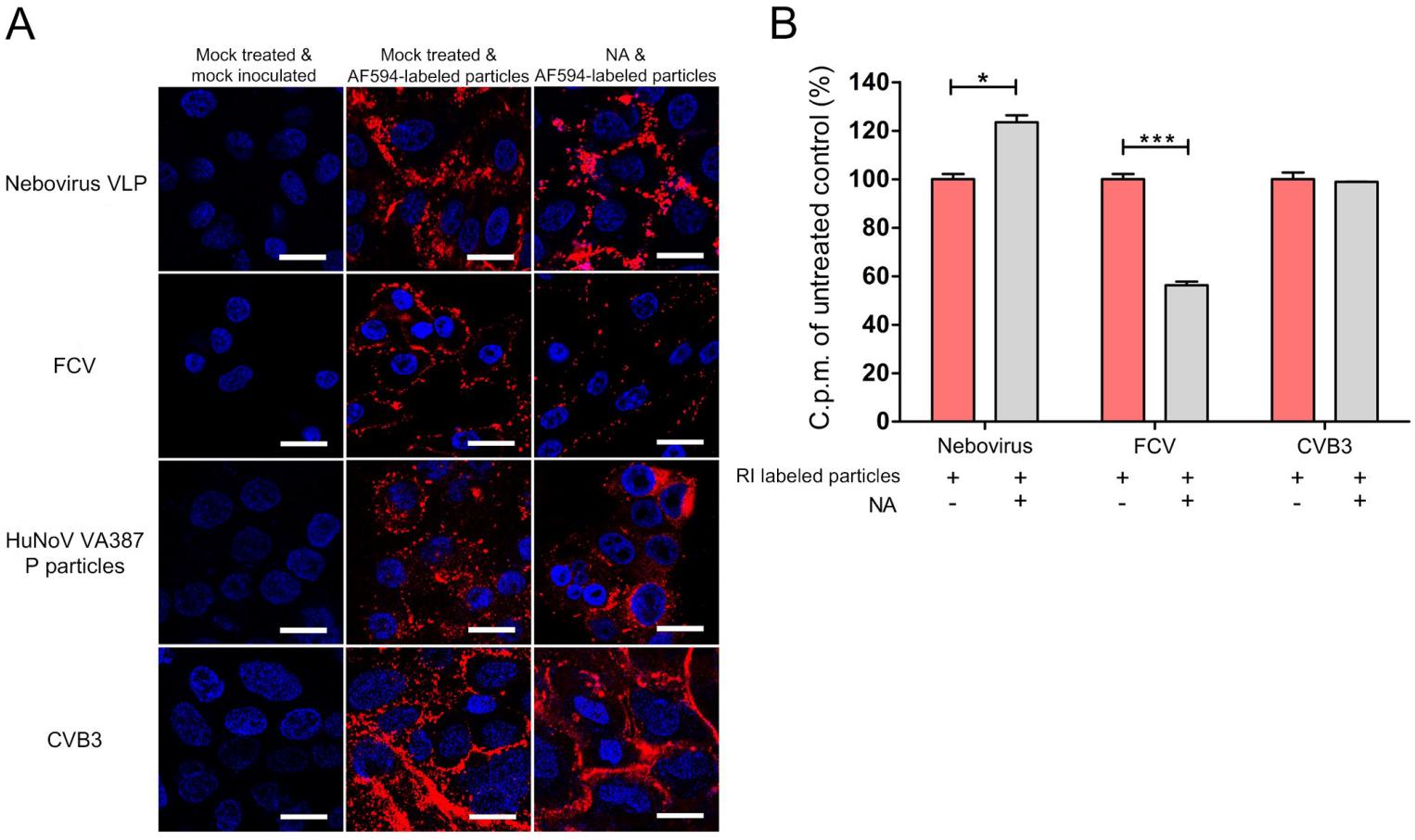
A
Mock treated & mock inoculated
Mock treated & AF594-labeled particles
NA & AF594-labeled particles
Nebovirus VLP
FCV
HuNoV VA387 P particles
CVB3
B
C.p.m. of untreated control (%)
140
120
100
80
60
40
20
0
*
***
Nebovirus
FCV
CVB3
RI labeled particles
NA

A

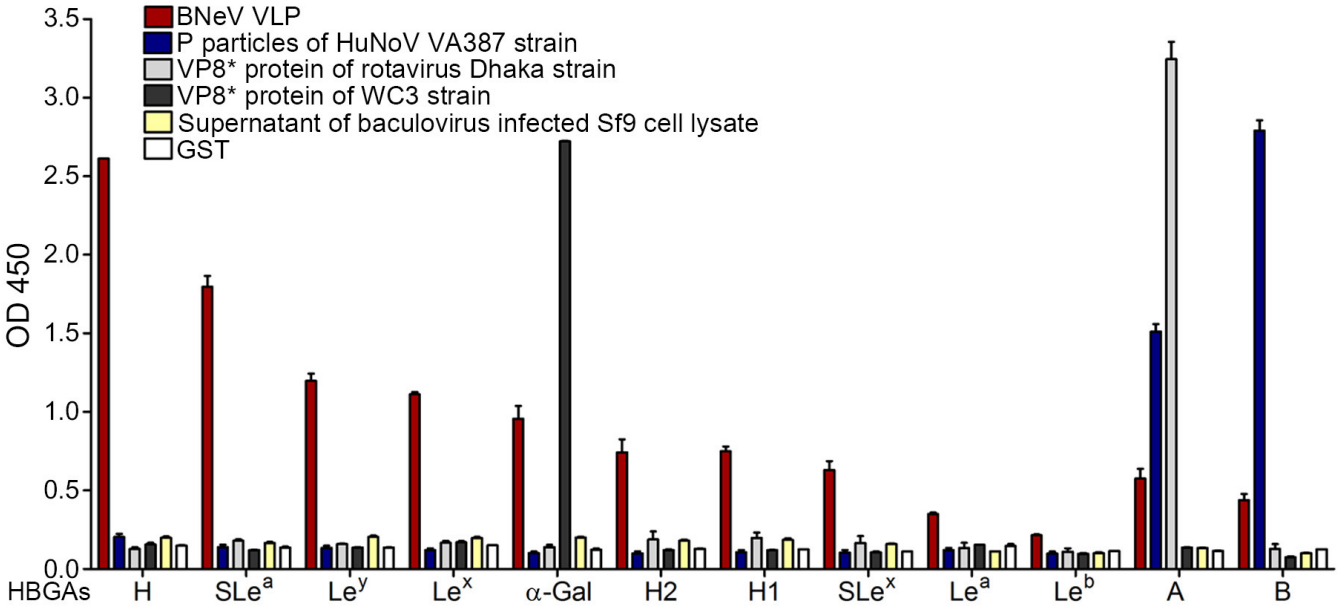

B

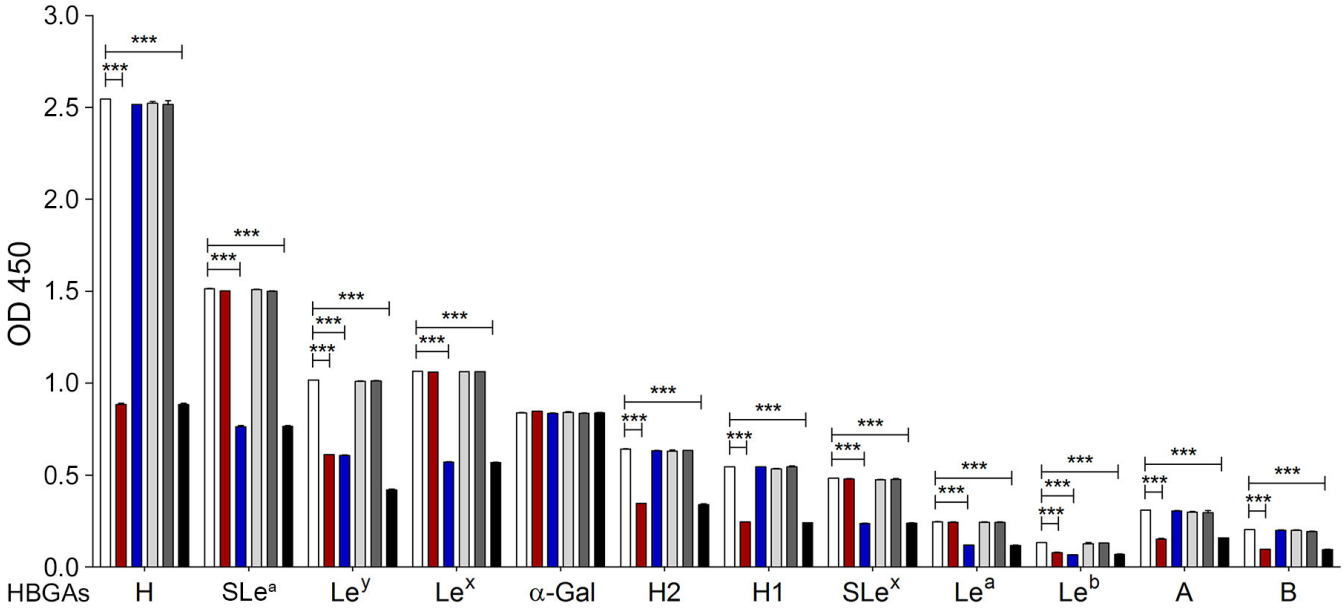

	H	SLe^a	Le^y	Le^x	α-Gal	H2	H1	SLe^x	Le^a	Le^b	A	B
BNeV VLP	+	+	+	+	+	+	+	+	+	+	+	+
α1,2-fucosidase	−	+	−	+	−	+	−	+	−	+	−	+
α1,3/4-fucosidase	−	−	+	+	−	−	+	+	−	−	+	+
α-galactosidase	−	−	−	−	+	+	−	−	+	+	−	−
αN-acetylgalactosaminidase	−	−	−	−	−	−	−	−	−	−	+	+

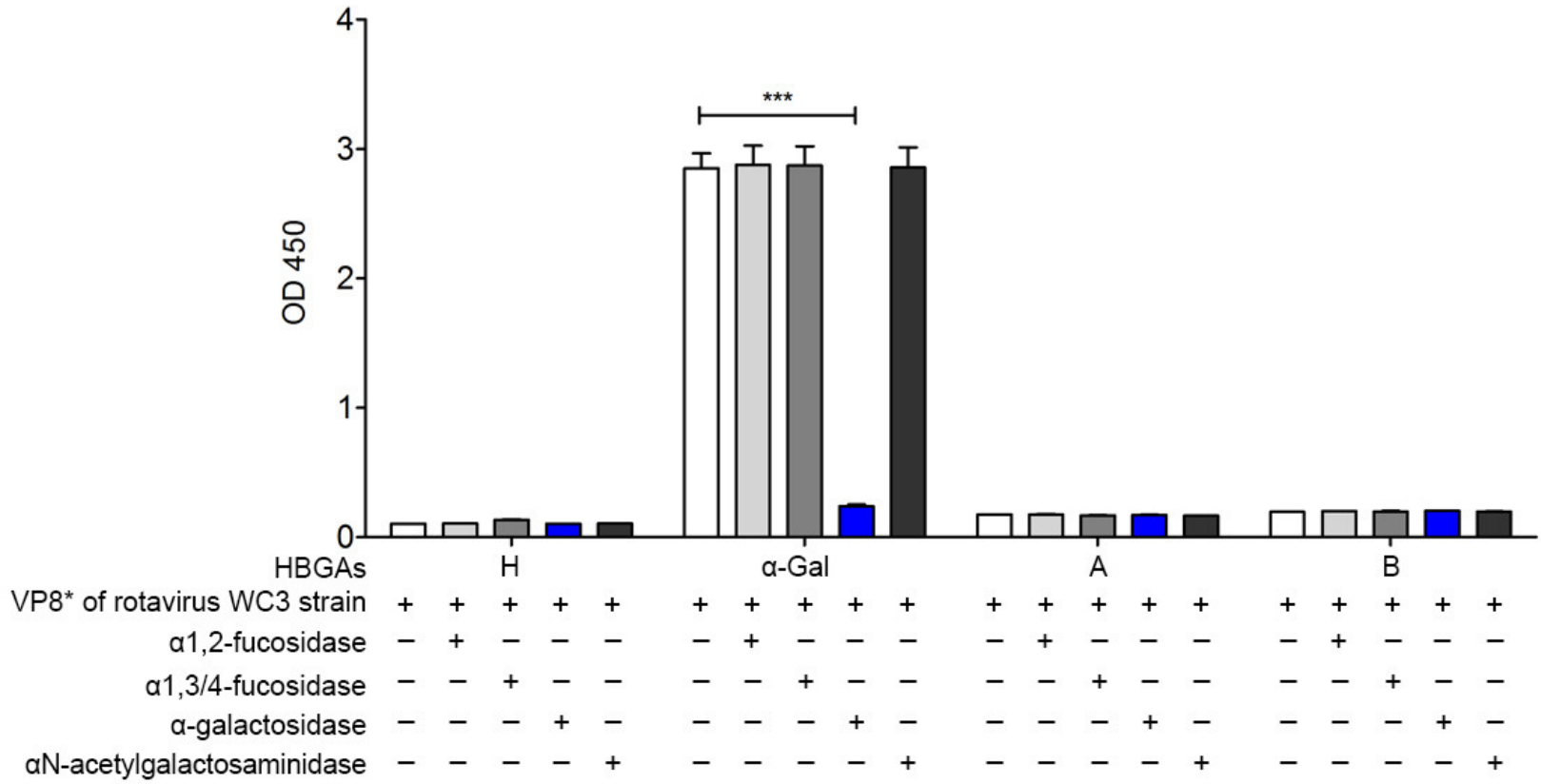
4
3
2
1
0
OD 450
***
HBGAs
H
α-Gal
A
B
VP8* of rotavirus WC3 strain +
α1,2-fucosidase − + − − − − + − − − − + − − − − + − − −
α1,3/4-fucosidase − − + − − − − + − − − − + − − − − + − −
α-galactosidase − − − + − − − − + − − − − + − − − − + −
αN-acetylgalactosaminidase − − − − + − − − − + − − − − + − − − − +

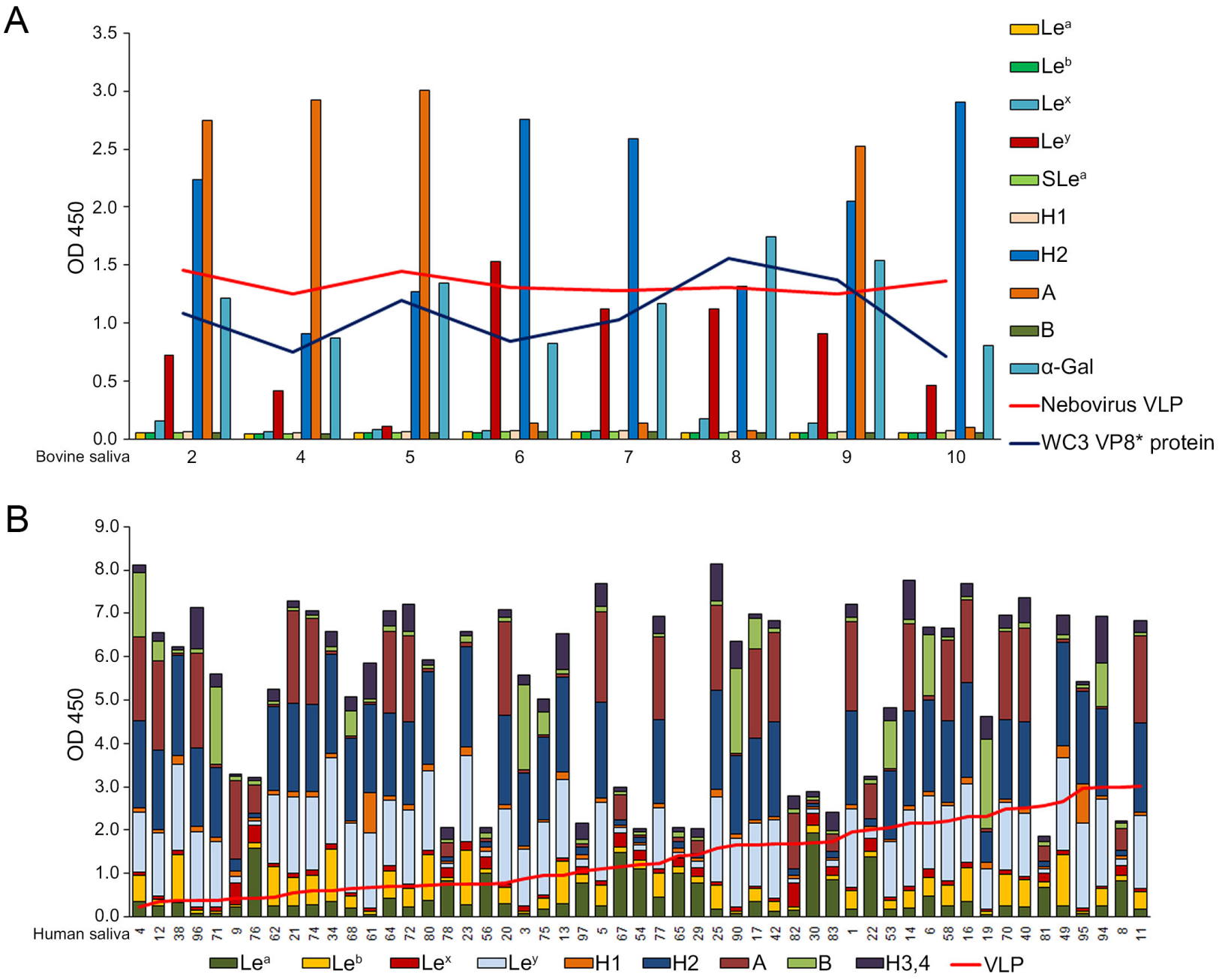
A
OD 450
3.5
3.0
2.5
2.0
1.5
1.0
0.5
0.0
Bovine saliva
2
4
5
6
7
8
9
10
Le^a
Le^b
Le^x
Le^y
SLe^a
H1
H2
A
B
α-Gal
Nebovirus VLP
WC3 VP8* protein
B
OD 450
9.0
8.0
7.0
6.0
5.0
4.0
3.0
2.0
1.0
0.0
Human saliva
4 12 38 96 71 9 76 62 21 74 34 68 61 64 72 80 78 23 56 20 3 75 13 97 5 67 54 77 65 29 25 90 17 42 82 30 83 1 22 53 14 6 58 16 19 70 40 81 49 95 94 8 11
Le^a
Le^b
Le^x
Le^y
H1
H2
A
B
H3,4
VLP

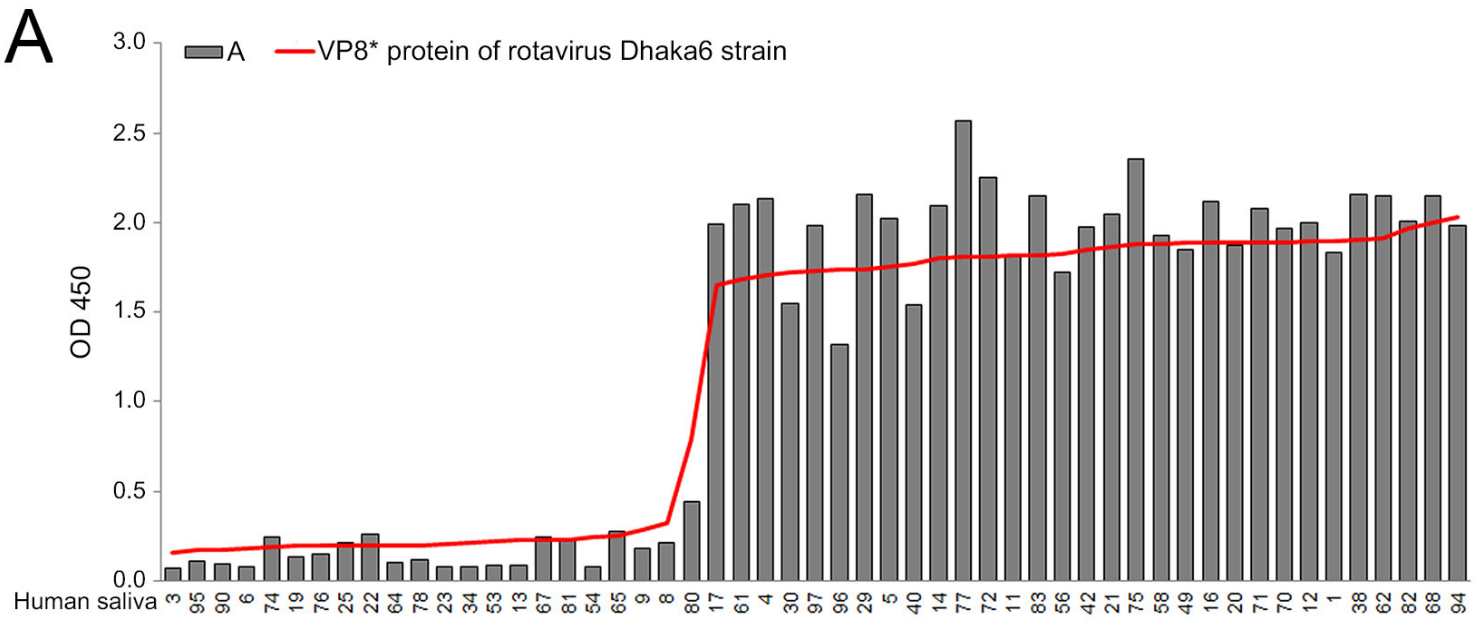
A
A
VP8* protein of rotavirus Dhaka6 strain
OD 450
3.0
2.5
2.0
1.5
1.0
0.5
0.0
Human saliva
3 95 90 6 74 19 76 25 22 64 78 23 34 53 13 67 81 54 65 9 8 80 17 61 4 30 97 96 29 5 40 14 77 72 11 83 56 42 21 75 58 49 16 20 71 70 12 1 38 62 82 68 94

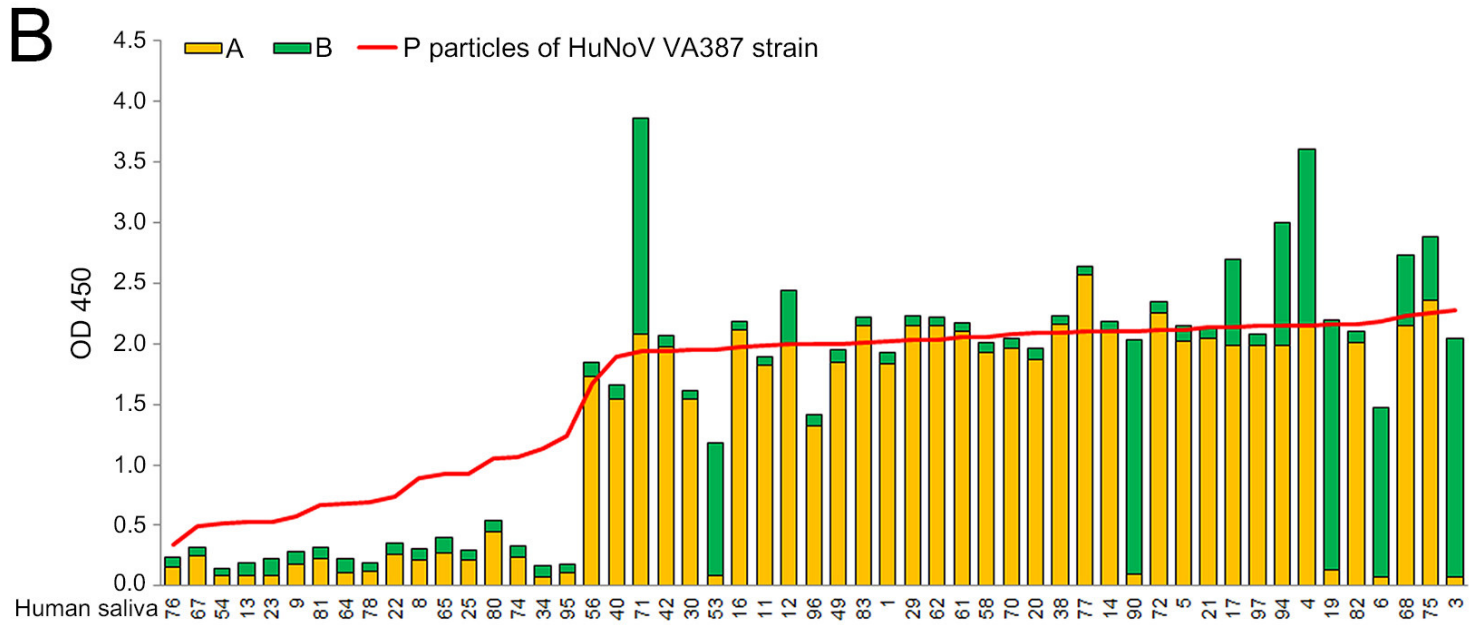
B
A
B
P particles of HuNoV VA387 strain
OD 450
4.5
4.0
3.5
3.0
2.5
2.0
1.5
1.0
0.5
0.0
Human saliva
76 67 54 13 23 9 81 64 78 22 8 65 25 80 74 34 95 56 40 71 42 30 53 16 11 12 96 49 83 1 29 62 61 58 70 20 38 77 14 90 72 5 21 17 97 94 4 19 82 6 68 75 3

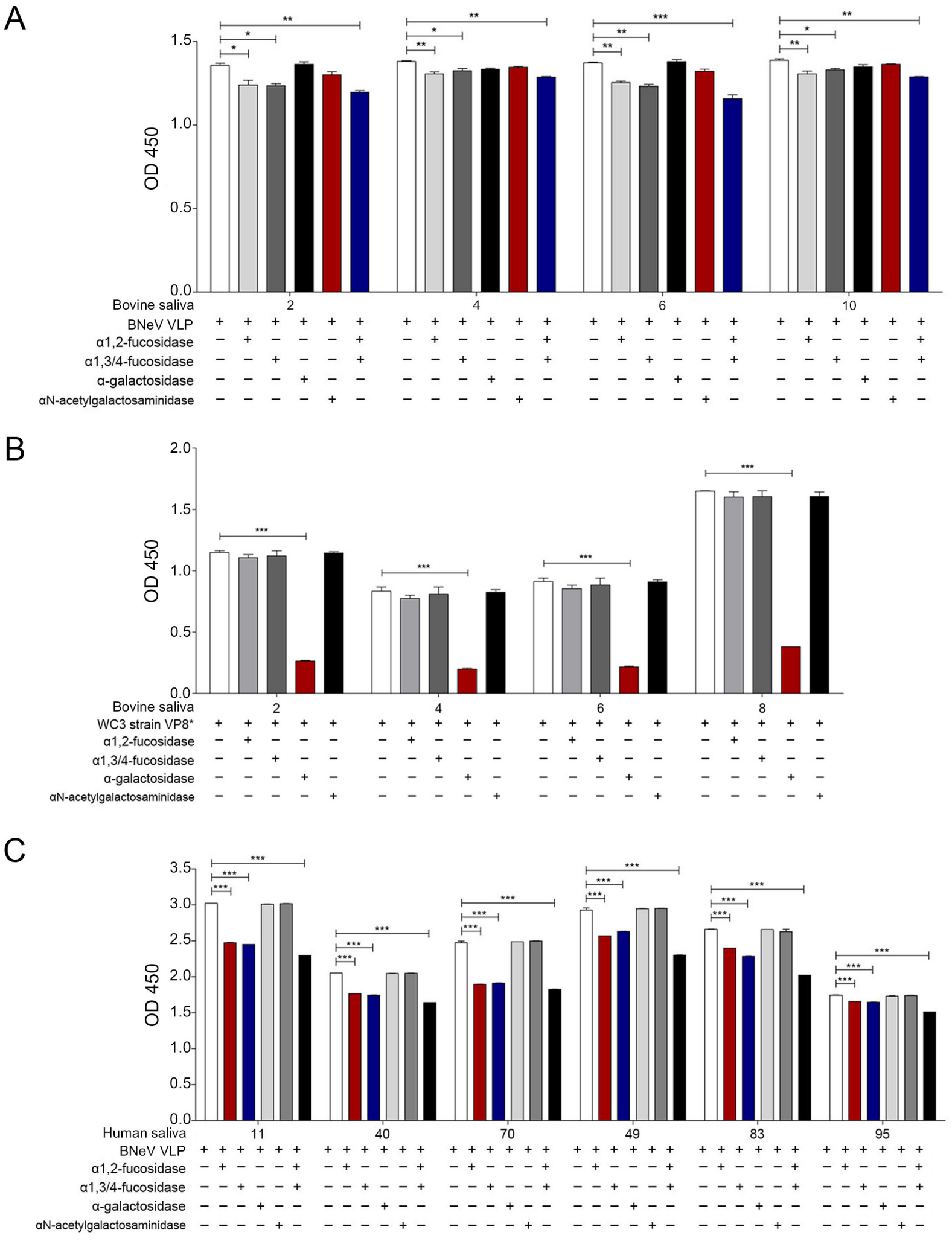
A
OD 450
1.5
1.0
0.5
0.0
Bovine saliva
2
4
6
10
BNeV VLP
α1,2-fucosidase
α1,3/4-fucosidase
α-galactosidase
αN-acetylgalactosaminidase
B
OD 450
2.0
1.5
1.0
0.5
0.0
Bovine saliva
2
4
6
8
WC3 strain VP8*
α1,2-fucosidase
α1,3/4-fucosidase
α-galactosidase
αN-acetylgalactosaminidase
C
OD 450
3.5
3.0
2.5
2.0
1.5
1.0
0.5
0.0
Human saliva
11
40
70
49
83
95
BNeV VLP
α1,2-fucosidase
α1,3/4-fucosidase
α-galactosidase
αN-acetylgalactosaminidase

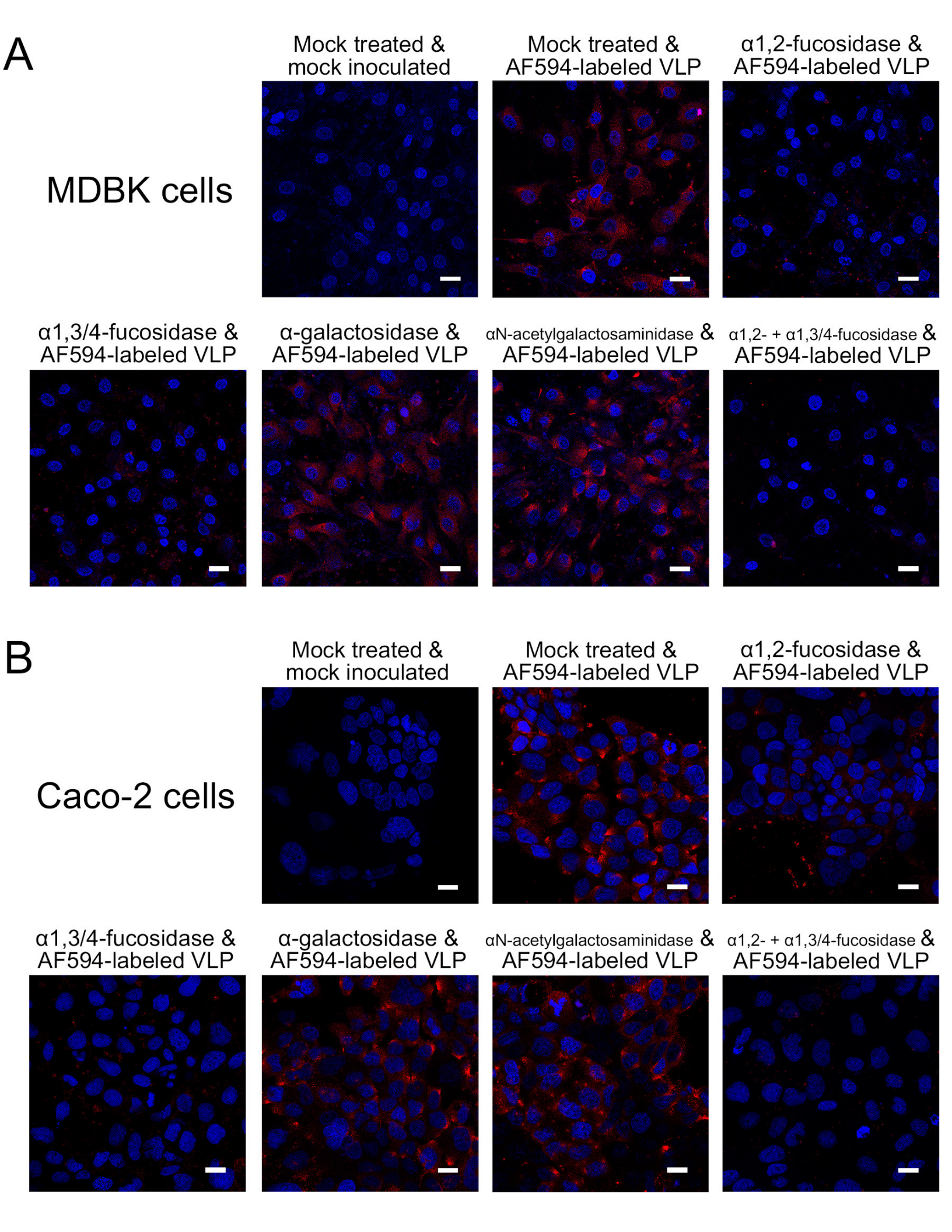
A
MDBK cells
Mock treated & mock inoculated
Mock treated & AF594-labeled VLP
α1,2-fucosidase & AF594-labeled VLP
α1,3/4-fucosidase & AF594-labeled VLP
α-galactosidase & AF594-labeled VLP
αN-acetylgalactosaminidase & AF594-labeled VLP
α1,2- + α1,3/4-fucosidase & AF594-labeled VLP
B
Caco-2 cells
Mock treated & mock inoculated
Mock treated & AF594-labeled VLP
α1,2-fucosidase & AF594-labeled VLP
α1,3/4-fucosidase & AF594-labeled VLP
α-galactosidase & AF594-labeled VLP
αN-acetylgalactosaminidase & AF594-labeled VLP
α1,2- + α1,3/4-fucosidase & AF594-labeled VLP

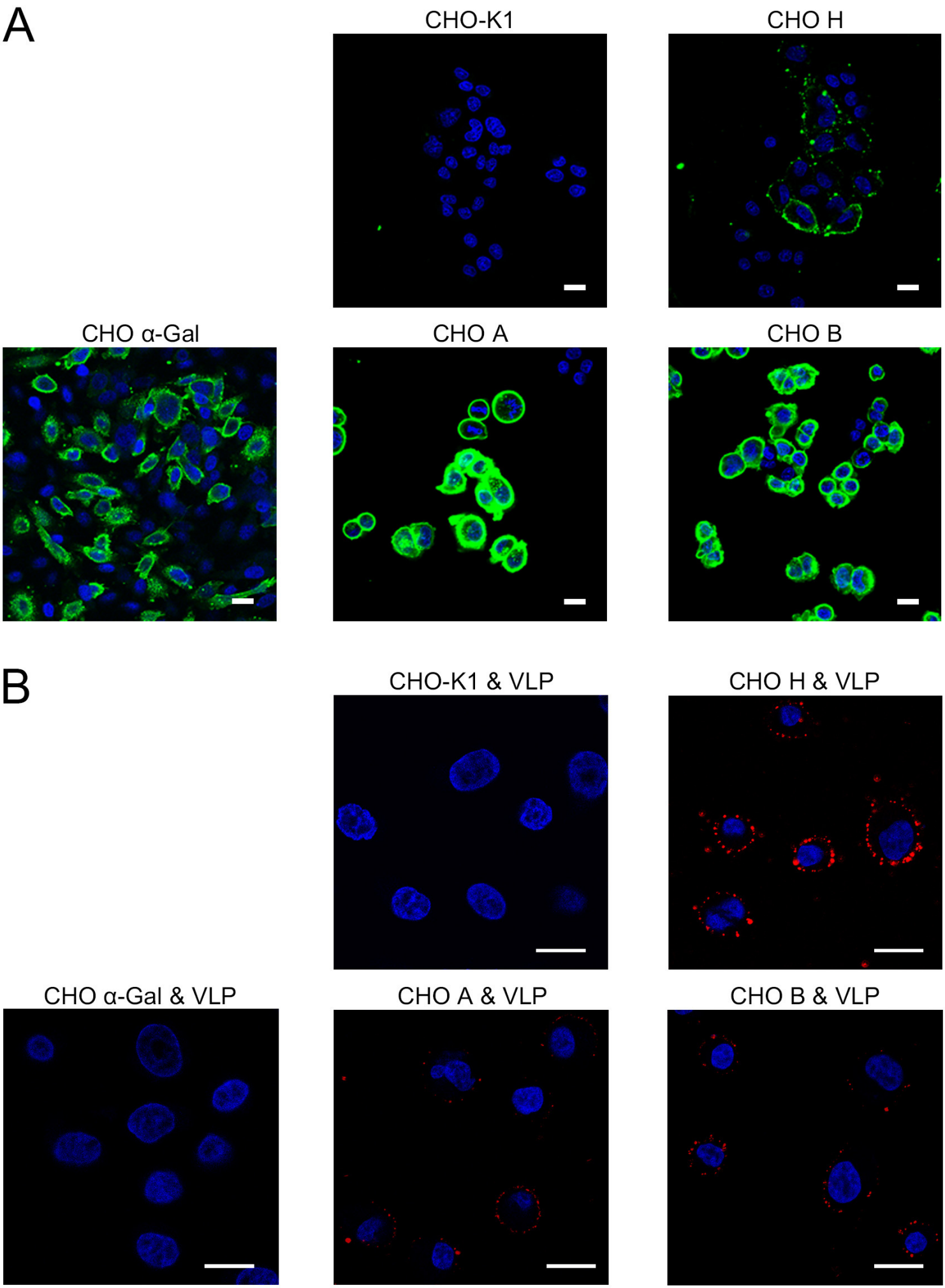
A
CHO-K1
CHO H
CHO α-Gal
CHO A
CHO B
B
CHO-K1 & VLP
CHO H & VLP
CHO α-Gal & VLP
CHO A & VLP
CHO B & VLP

A

(H+/A+/B-)

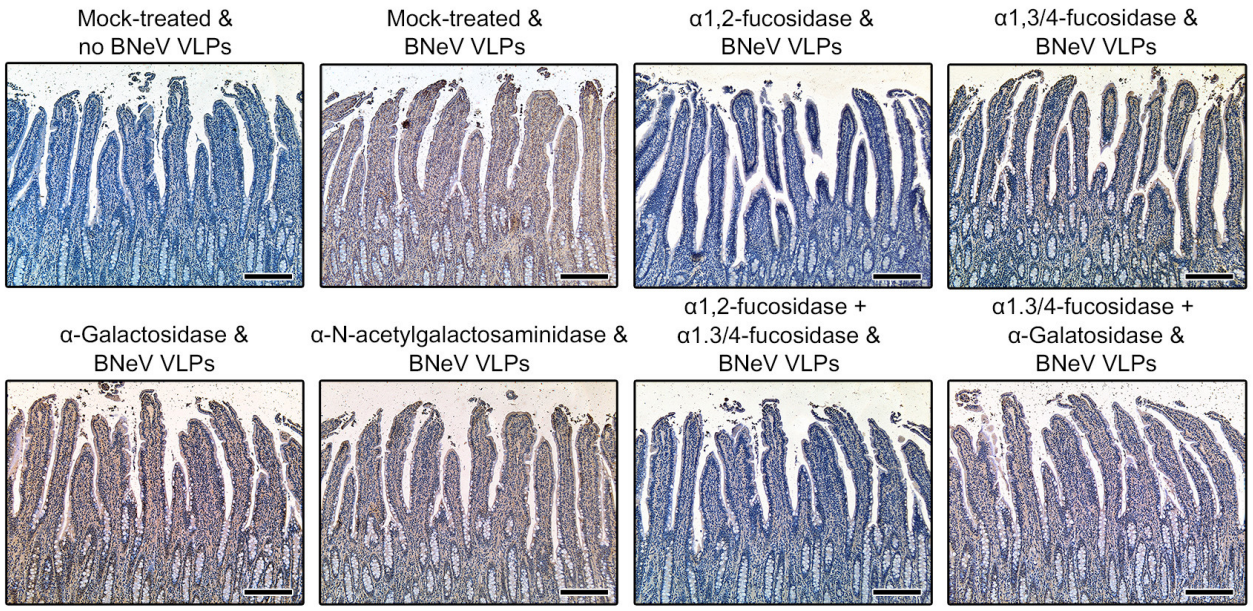
Mock-treated &
no BNeV VLPs
Mock-treated &
BNeV VLPs
α1,2-fucosidase &
BNeV VLPs
α1,3/4-fucosidase &
BNeV VLPs
α-Galactosidase &
BNeV VLPs
α-N-acetylgalactosaminidase &
BNeV VLPs
α1,2-fucosidase +
α1.3/4-fucosidase &
BNeV VLPs
α1.3/4-fucosidase +
α-Galatosidase &
BNeV VLPs

B

(H+/A-/B-)

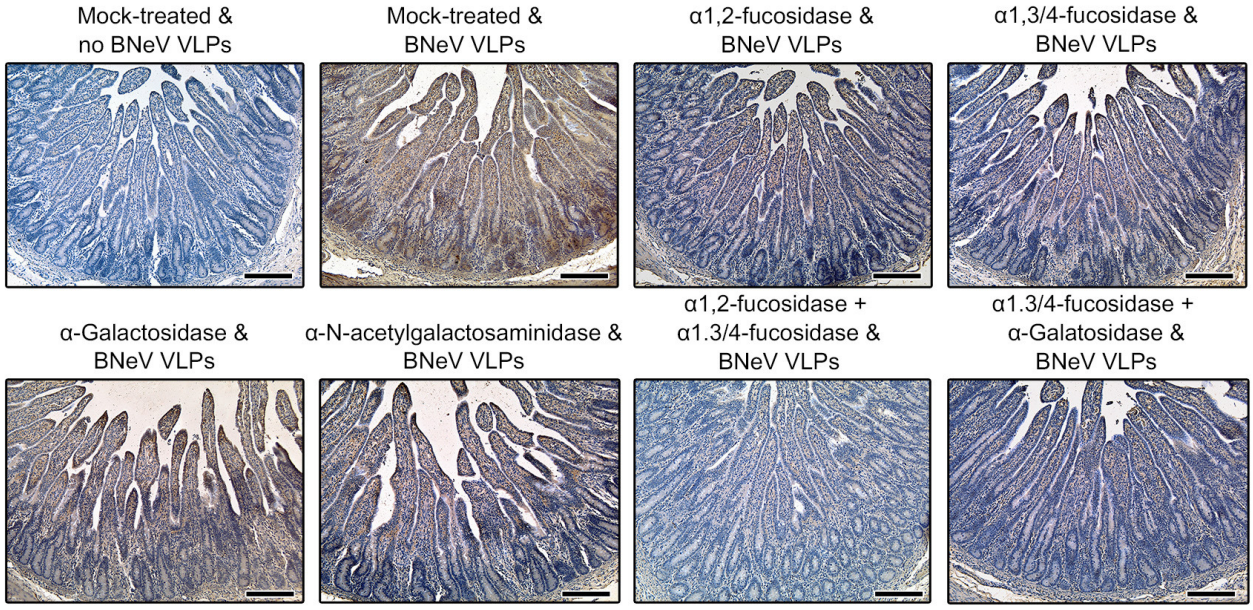
Mock-treated &
no BNeV VLPs
Mock-treated &
BNeV VLPs
α1,2-fucosidase &
BNeV VLPs
α1,3/4-fucosidase &
BNeV VLPs
α-Galactosidase &
BNeV VLPs
α-N-acetylgalactosaminidase &
BNeV VLPs
α1,2-fucosidase +
α1.3/4-fucosidase &
BNeV VLPs
α1.3/4-fucosidase +
α-Galatosidase &
BNeV VLPs